Journal of Geophysical Research – Solid Earth

Supporting Information for

Earthquake Supercycles on the Mentawai Segment of the Sunda Megathrust in the 17th Century and Earlier

B. Philibosian[1†], K. Sieh[2], J.-P. Avouac[1], D. H. Natawidjaja[3], H.-W. Chiang[4], C.-C. Wu[4], C.-C. Shen[4], M. R. Daryono[5], H. Perfettini[1‡], B. W. Suwargadi[3], Y. Lu[2], and X. Wang[2]

[1]Tectonics Observatory, Division of Geological and Planetary Sciences, California Institute of Technology, Pasadena, California. [2]Earth Observatory of Singapore, Nanyang Technological University, Singapore. [3]Research Center for Geotechnology, Indonesian Institute of Science (LIPI), Kampus LIPI Bandung, Bandung, Java, Indonesia. [4]High-Precision Mass Spectrometry and Environment Change Laboratory (HISPEC), Department of Geosciences, National Taiwan University, Taipei, Taiwan ROC. [5]Institut Teknologi Bandung, Bandung, Java, Indonesia. [†]Now at U.S. Geological Survey, Menlo Park. [‡]Now at IRD/ISTerre, Université Joseph Fourier, Grenoble, France.

Contents of this file

Additional Supporting Information (Files uploaded separately)

Introduction

Site maps and cross sections for all sites and coral samples not featured in the main text of the paper. Additional descriptions of Cimpungan coral samples and Pasapuat site & samples. Figures showing alternative coseismic models and expanded modeling results such as model spatial resolution and residuals. Tables of U-Th disequilibrium dating analyses and of model moments and misfits.

Text S1.

Description of additional microatoll cross sections from Cimpungan

In addition to the three presented in the main text, we sampled seven other microatolls at Cimpungan. Figure S1 shows two with primarily cup-shaped morphology, CMP08-B2 and B3. We collected a complete diameter from B2 (rather than a customary radius) to illuminate its unusual inner growth history, which clearly shows that the microatoll tilted in ~1569. The tilting was coincident with a particularly large die-down which is apparent on most of the corals at this site. After many years of subsidence, B2 experienced its first uplift in 1597 and began to form a hat shape. Some parts of the perimeter died in 1607, such as the left side of this cross section, perhaps due to stress of the shallowing lagoon. The colony was killed completely by the larger sudden uplift in 1613.

CMP08-B3 is one of the few truly cup-shaped microatolls from this site. The dates are quite imprecise, leaving uncertainty as to whether this coral grew during the period of submergence in the late 1500s or the late 1600s. Its morphology indicates it cannot have grown during the period of emergence in the early 1600s which is well-defined by the hat-shaped microatolls. We infer that it grew during the earlier submergence period, as it appeared to be part of the same population as B2 and exhibits a notable die-down which plausibly corresponds to the 1569 event. The outer perimeter of B3 is thin and significantly eroded, so it is plausible that this microatoll died due to the 1597 uplift.

Figure S2 shows cross sections of two more primarily cup-shaped microatolls from Cimpungan site C. Both of these record long histories of interseismic subsidence during the mid to late 1500s leading up to the emergence period. The upper surfaces of the outer perimeters of both corals are significantly eroded, obscuring the effects of the small 1597 uplift. Both of these corals apparently died in about 1607. They may have died due to stress as the lagoon continued to shallow between 1597 and 1613, or they may actually have died due to uplift in 1613 and have been somewhat eroded.

Figure S3 shows cross sections of three additional hat-shaped microatolls from Cimpungan sites A and B, which help to further define the early-1600s emergence period. CMP08-A1 was overturned early in its life, the 20-cm diameter head easily rolled by storm waves. For the next 30 years the head recorded subsidence, followed by another ~30 years of emergence defined by lowering concentric rings (though the eroded surface does not preserve the individual die-downs). CMP08-A3 has a growth history very similar to A1, except that the major uplift events somewhat more clearly occurred in 1597 and 1611. A1 and A3 both clearly show the large 1569 die-down. CMP08-B5, a Favid, provides the tightest age constraints on the emergence period as it records the 1597 uplift and subsequent uplift continuing until it died in ~1609. It is possible that it actually died in 1613 (the annual bands become very fine and hard to discern), or that the very thin living outer perimeter simply died due to stress.

Description of Pasapuat Site and Microatoll Samples

Pasapuat is a village on the northeast coast of North Pagai. At our nearby study site, the intertidal reef platform is covered with dozens of fossil microatolls, well-preserved close to the beach and more eroded farther seaward (Figure S11). A peat layer which crops out beneath the beach probably originally covered most or all of the microatolls and protected them from erosion. As at many other sites, this peat and the trees that grew in it must have formed after

a tectonic uplift raised the coral platform above sea level. Tectonic subsidence has since drowned the trees and led to the erosion of the peat.

We collected slabs from seven microatolls at Pasapuat, three of which were presented and discussed in previous papers. Here we present the remaining four microatolls, which record a complex tectonic history during the 16th and 17th centuries. The youngest of these, PSP08-B1 (Figure S12A), was overturned and transported into significantly deeper water in about 1658, when its diameter was already at least 40 cm. This event suggests a tsunami, as it is unlikely that storm waves could have overturned and transported such a large piece of coral. After growth reached HLS again in 1678, the coral experienced slow submergence until a significant uplift killed the colony in about 1703.

A somewhat older microatoll, PSP08-B3 (Figure S12B), recorded a more complex tectonic history comprising a period of stability (1537–1554), a period of submergence (1554–1584), and a period of emergence (1584–1626). There was a final short period of submergence before the colony was killed in ~1631 by uplift. A small Favid microatoll, PSP08-B4 (Figure S12C), which was embedded in the outer perimeter of B3, provides a better age constraint for the death of both colonies, supporting the conclusion that the uplifts at this site were contemporaneous with those at Cimpungan (1597, 1613, and 1631). The 1613 die-down is preserved on B3, whereas the inferred 1597 die-down has been eroded.

The largest microatoll, PSP08-B2 (Figure S13A), has a broad hat shape indicating a ~35-year period of emergence followed by a 70-year period of submergence. The weighted average of the three dates obtained for this specimen place the record at odds with the B3 record, with the emergence period on B2 corresponding to the submergence period on B3 and vice versa. We infer that the ages probably have larger uncertainties than stated, since the periods of emergence on the two microatolls were very likely contemporaneous. Our interpretation falls just within the uncertainty for two of the three dates and is outside for the third. As none of the U-Th age determinations for this specimen included successful isochron analyses, it is possible that these samples had unusually high initial thorium content, resulting in calculated ages a few decades older than the true age. According to our interpretation, the emergence period ended with a final uplift in 1631 which did not quite kill the coral. After an initial rapid submergence, subsidence continued at low rates until the coral was killed due to uplift in 1703.

Figure S13B shows the growth histories of all the Pasapuat microatolls with the B2 record shifted in time according to our interpretation. The complete tectonic deformation history is generally similar to the Cimpungan history. There is no evidence of uplift at this site that would correlate with the potential 1658 tsunami that overturned B1, but a tsunami generated farther north could easily have reached this site.

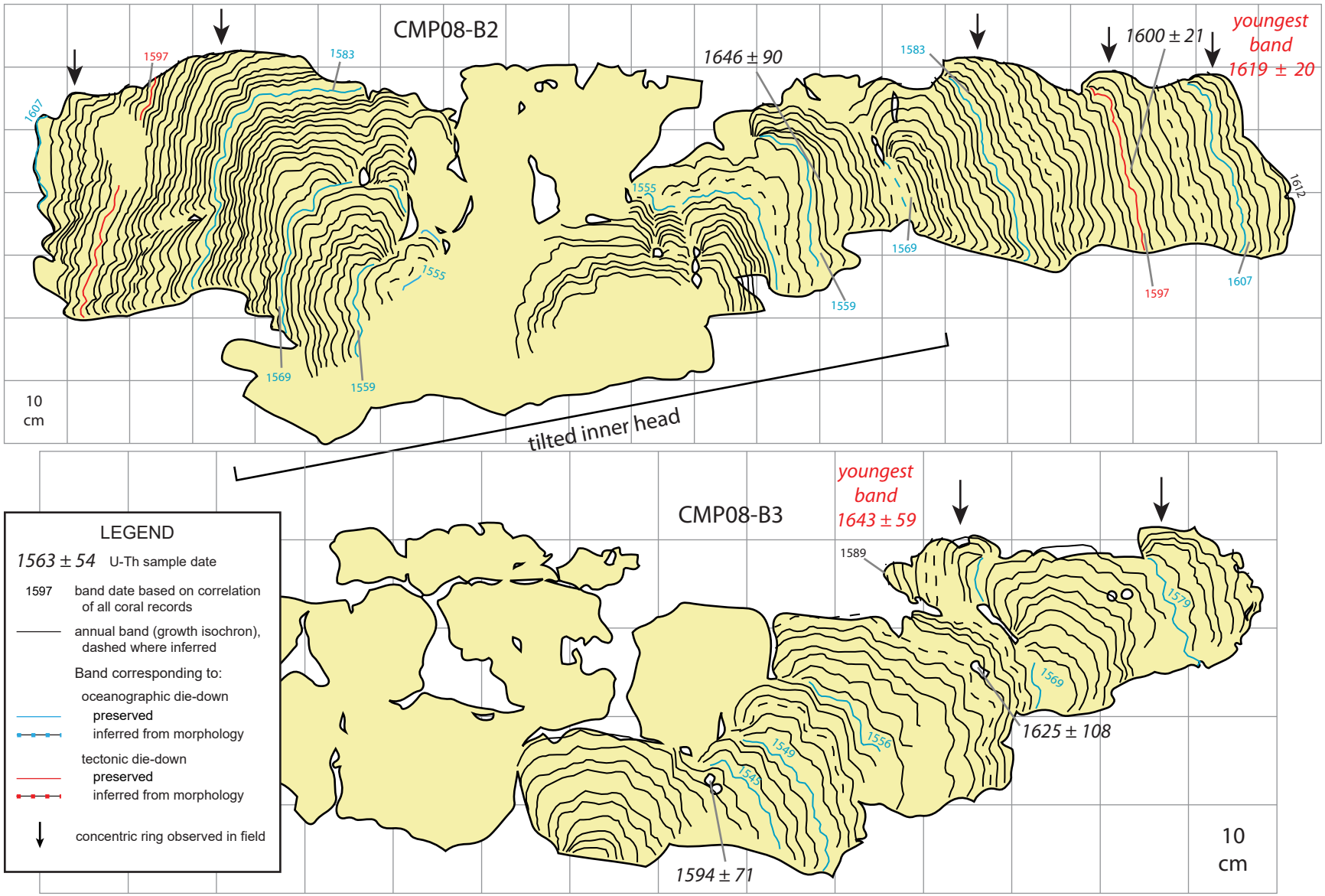

Figure S1. Cross sections of two primarily cup-shaped microatolls from Cimpungan which record longer histories leading up to the period of emergence. B2 tilted at the time of the large 1569 die-down which affected all the corals at this site.

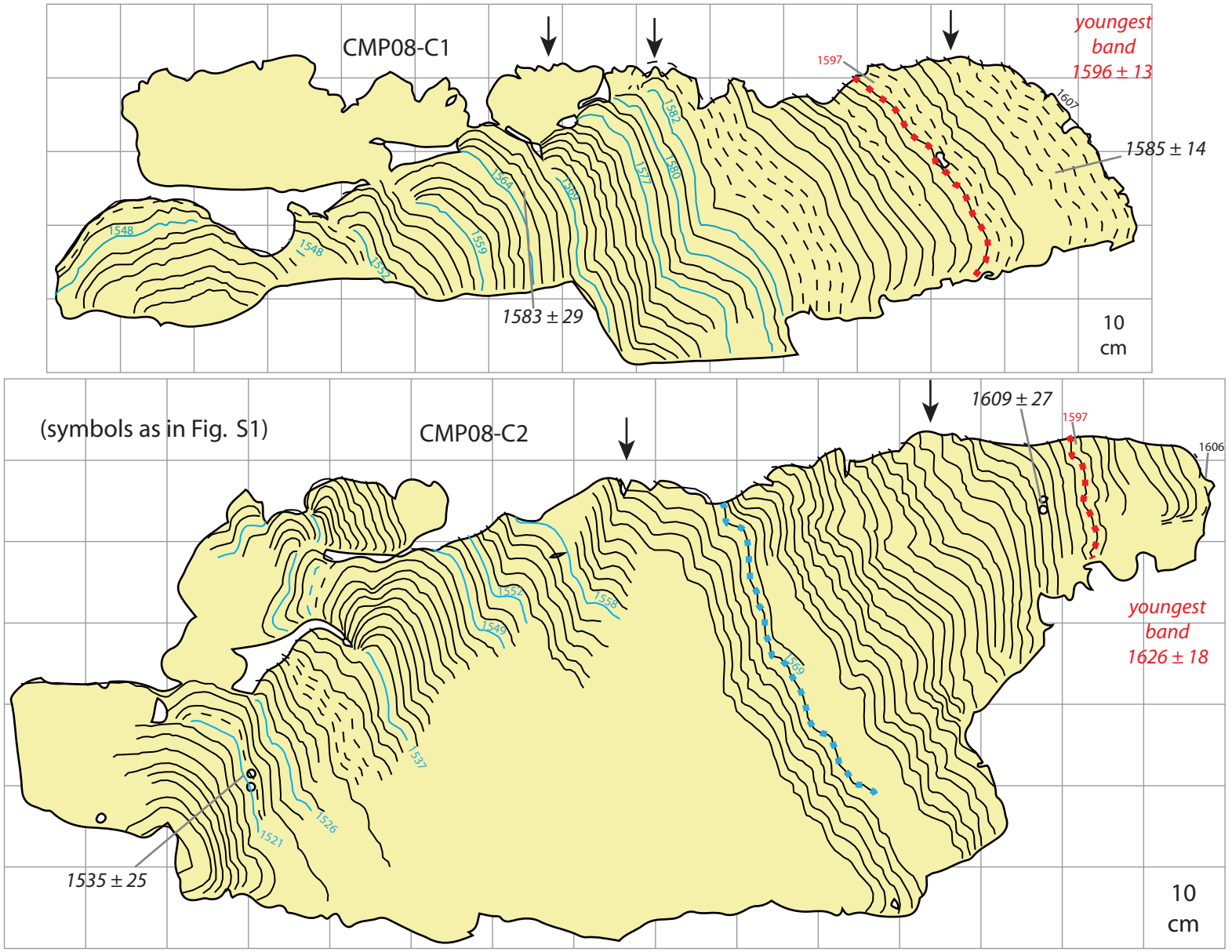

Figure S2. Cross sections of two cup-shaped microatolls from Cimpungan that record a long history of submergence prior to uplift.

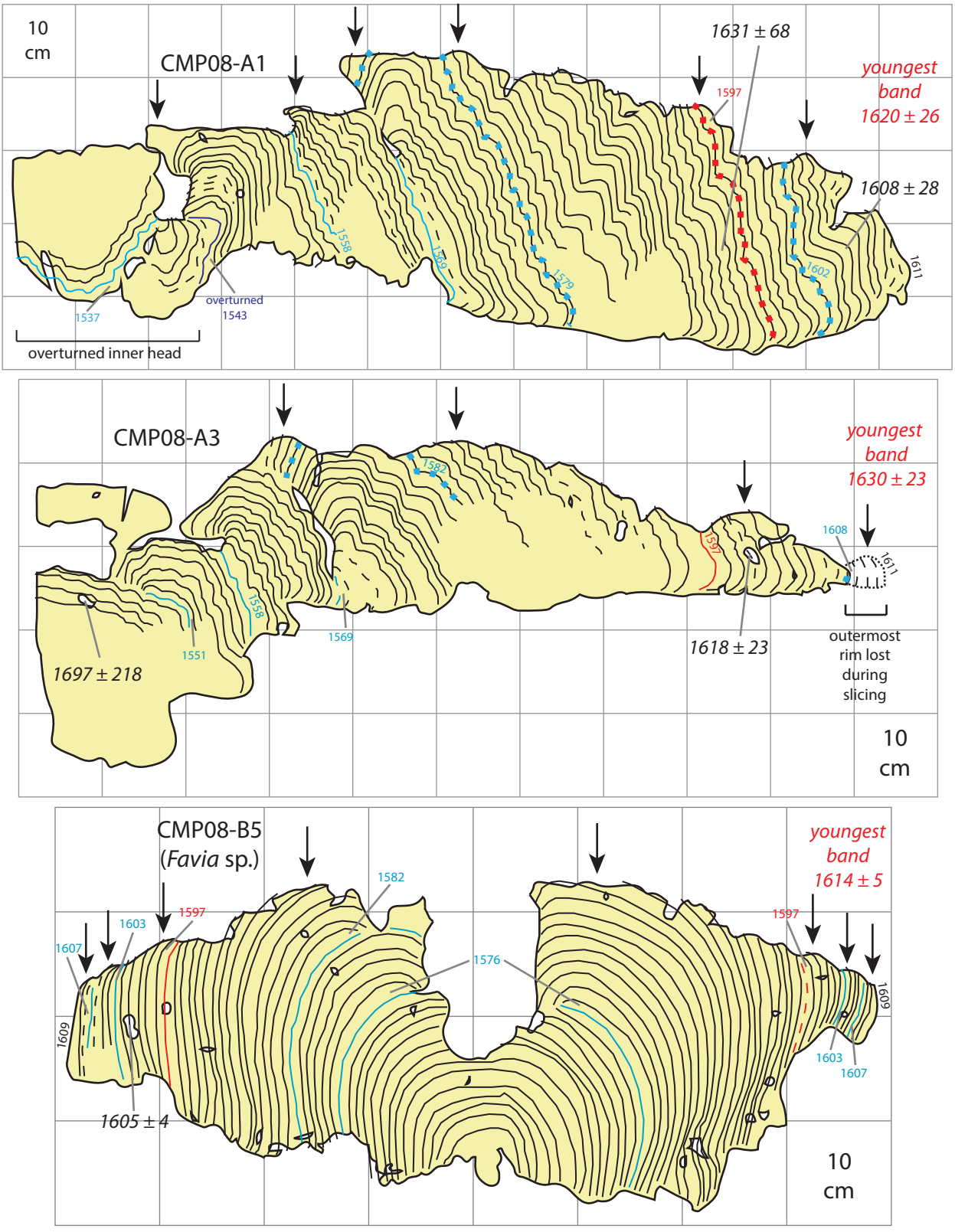

Figure S3. Cross sections of three hat-shaped microatolls from Cimpungan recording a period of submergence followed by a period of emergence, the latter likely punctuated by multiple sudden uplifts. Symbols as in Fig. S1.

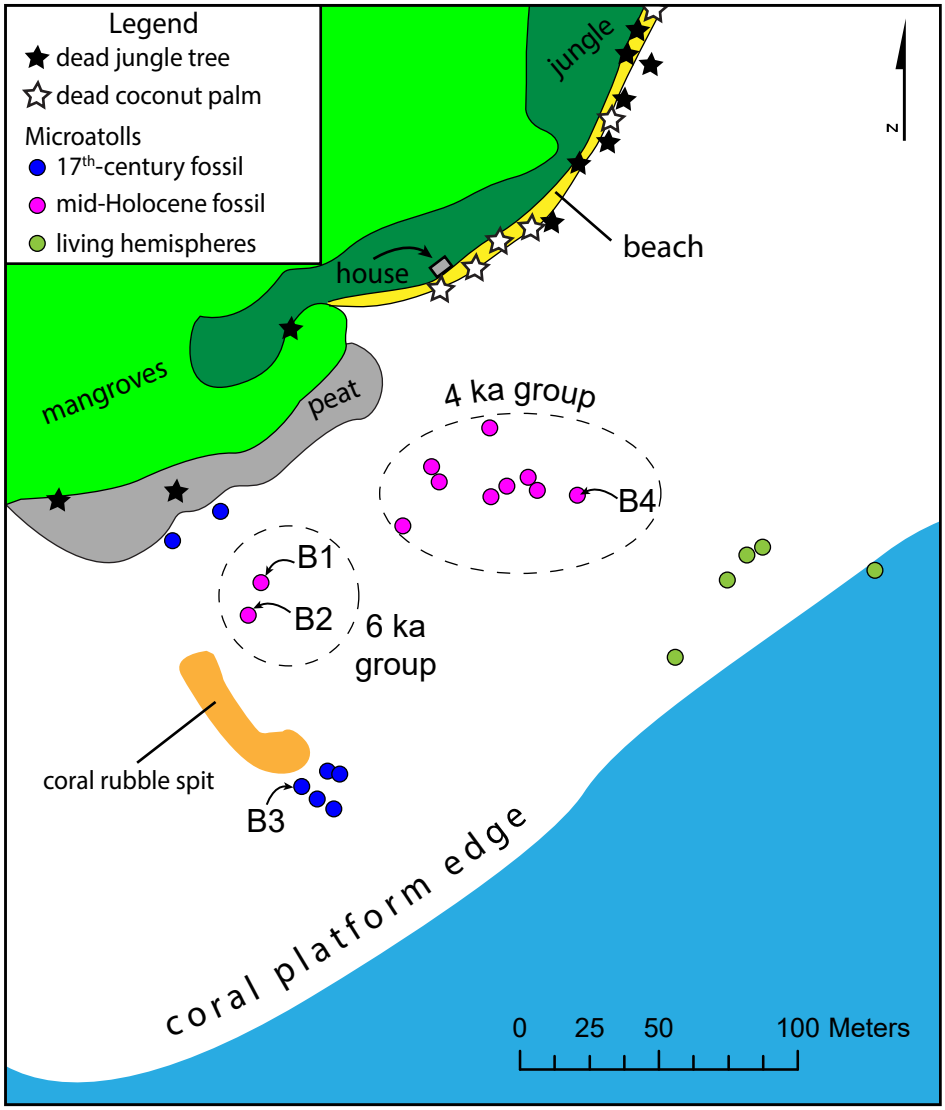

Figure S4. Map of Sarabua, a site on an islet in a large bay on the east coast of Siberut. Two populations of remarkably well-preserved mid-Holocene microatolls lie in the middle of the coral platform (dates discussed by *Philibosian et al.* [2012]). B3 comes from a population of *Goniastrea* microatolls that died in the 17th century. A peat layer and numerous dead trees along the beach are evidence of an ancient coseismic uplift and subsequent subsidence. Due to slow recovery from the extensive death of the reefs in this area during the catastrophic 1997–1998 IOD event and phytoplankton bloom [*Abram et al.* 2003], the living corals at this site in 2010 had not yet reached HLS and become microatolls.

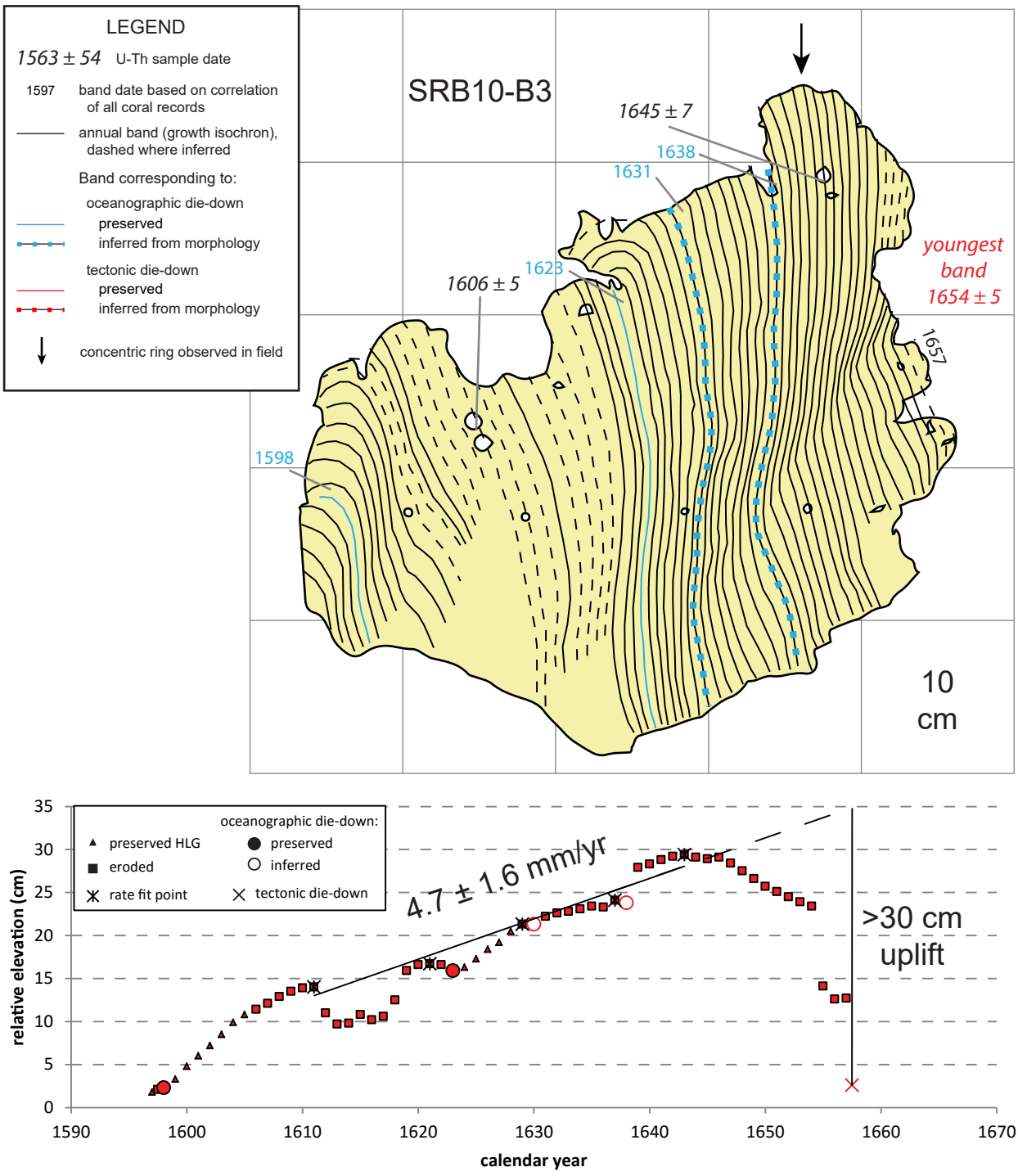

Figure S5. Cross section and growth history of SRB10-B3, a *Goniastrea sp.* microatoll from Sarabua. The coral experienced moderate interseismic subsidence for at least 50 years before dying in a presumed uplift in about 1658.

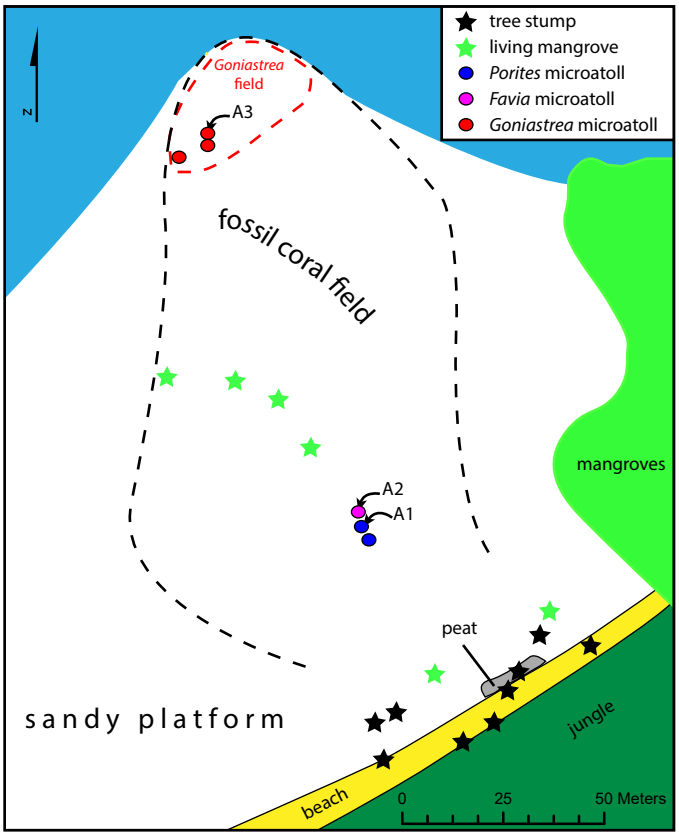

Figure S6. Data from Muara Siberut.

A) Map of Muara Siberut site on the east coast of Siberut. All the fossil corals at this site died in the 17th century. As at many other sites, remnants of a peat layer and stumps of jungle trees attest to a period when the coral platform was raised above the intertidal zone, and subsequent subsidence. A nearby stream outlet flooded this area with sand and prevented the growth of modern corals.

B) Radial cross section of MSB10-A3 and diameter cross section of MSB10-A2. One of the three dates obtained from A3 is inconsistent with the other two; we exclude the apparently erroneous 1675 ± 19 date from our analysis. The morphology and dates of A2 suggest that it grew contemporaneously with the interior of A3, but died for non-tectonic reasons. A3 was part of a well-defined population of fossil microatolls (suggesting death due to tectonic uplift) whereas A2 was more isolated.

C) Diameter cross section of MSB10-A1. The age uncertainty is extremely large, encompassing the 1797 and 1833 earthquakes as well as part of the 17th-century rupture sequence. However, its proximity and similarity to A2 leads us to infer that the two are about the same age.

D) Growth history plot of all three microatolls from Muara Siberut. A2 and A1 likely sank 10–15 cm into the substrate relative to A3 (they were found slightly tilted). A3 provides the longest and most reliable tectonic history for this site, recording ~50 years of moderate interseismic subsidence culminating in a sudden uplift of at least 30 cm.

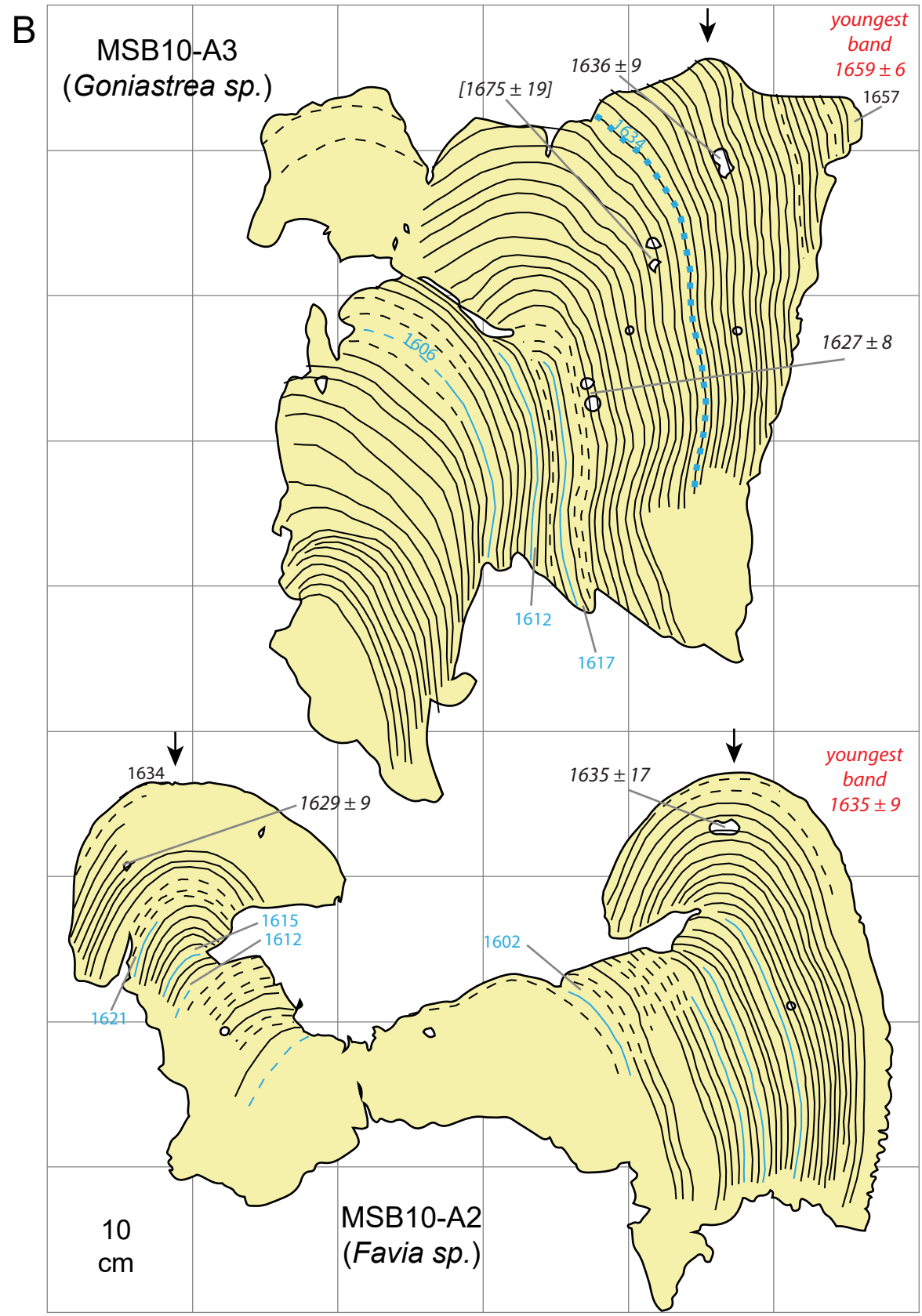

Figure S6 (continued). Symbols as in Fig. S5.

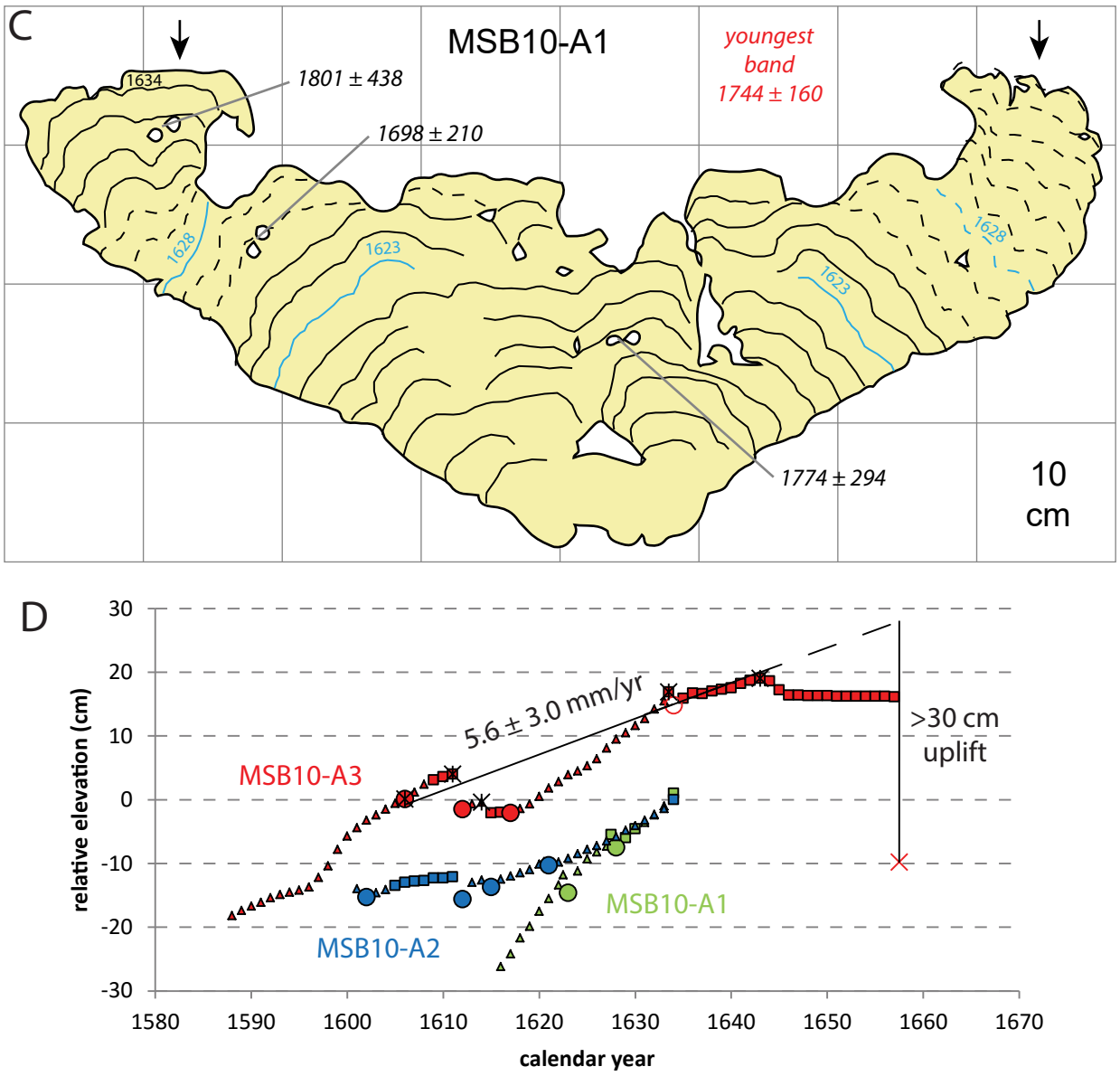

Figure S6 (continued). Symbols as in Fig. S5.

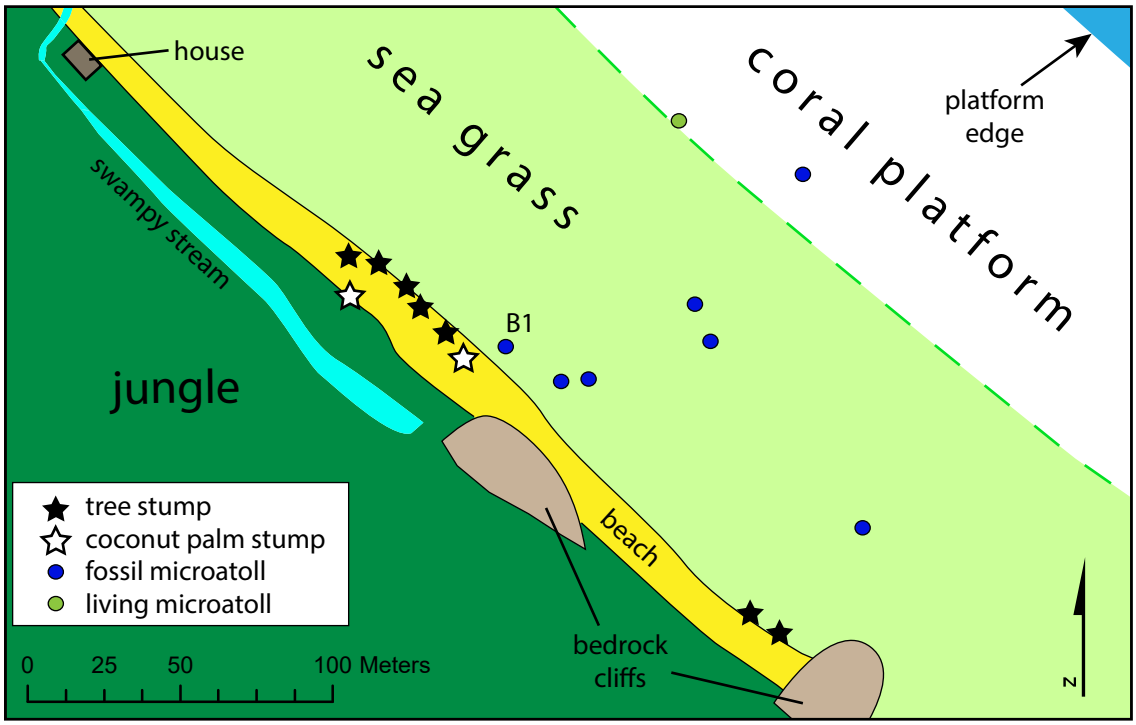

Figure S7. Map of Pulau Panjang site B, on a small island north of Sipora. Many tree stumps in the beach are evidence of recent interseismic subsidence. The single population of fossil corals at this site died in the late 16th century.

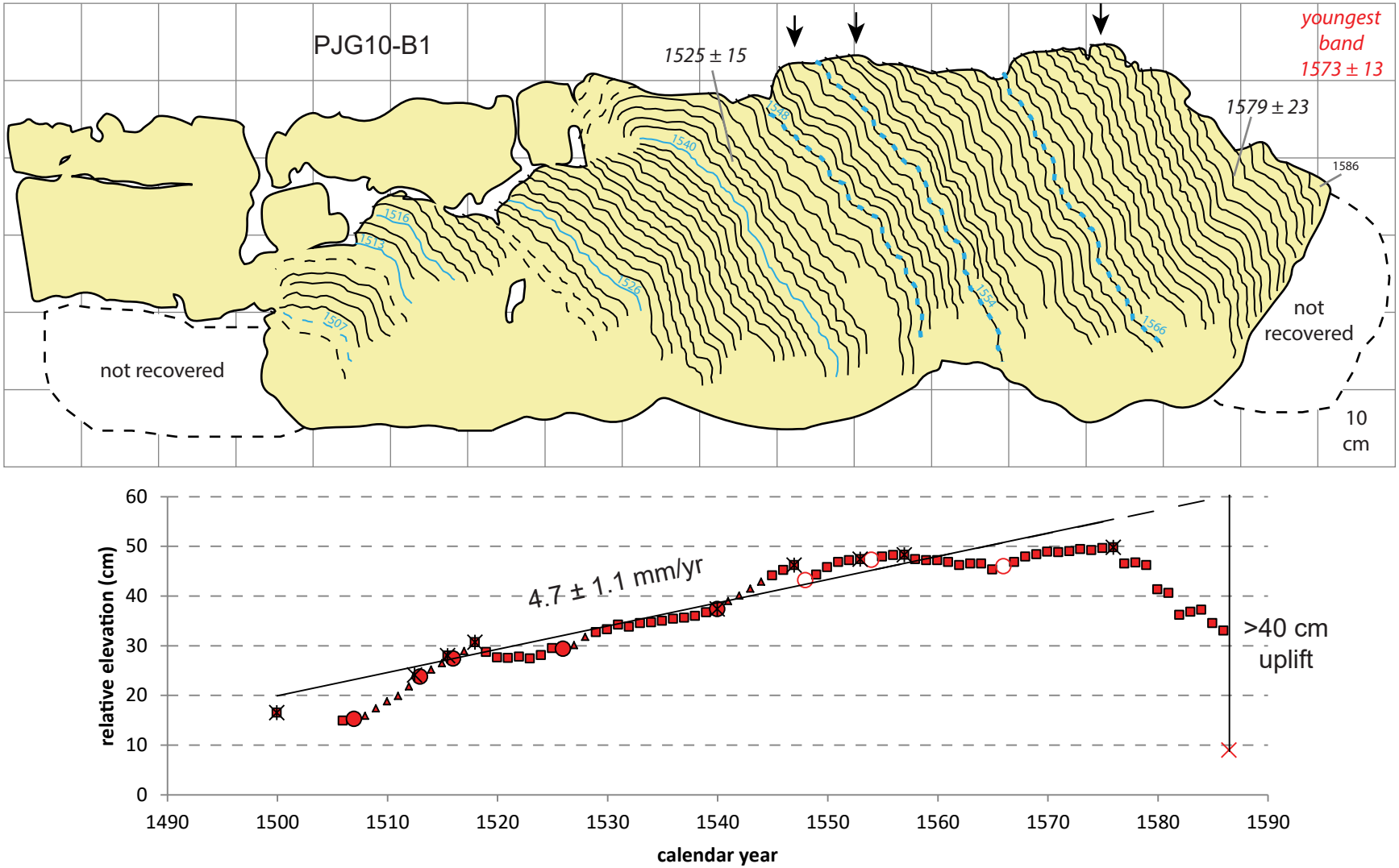

Figure S8. Cross section and growth history of PJG10-B1 from Pulau Panjang site B (symbols as in Fig. S5). The innermost and outermost portions of the slab were buried in deep sediment and could not be recovered. This microatoll experienced moderate interseismic subsidence for 80–90 years before being uplifted and killed in the late 1500s.

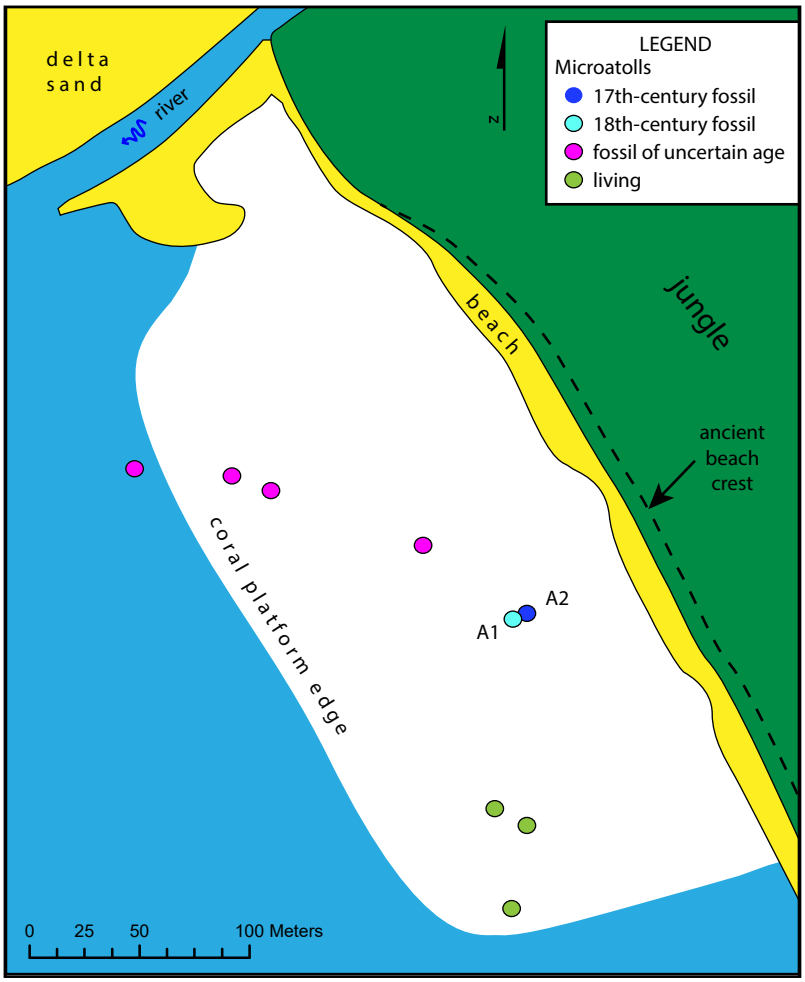

Figure S9. Map of North Pukarayat on the northwest coast of Sipora.. Most fossil microatolls at this location were tilted and eroded, so it is unclear whether they were the same generation as A1 or A2. A2 died in the 18th century and was discussed by *Philibosian et al.* [2014]; A1 died in the 17th century and has a hat shape indicating two uplift events. An ancient beach crest likely corresponds to one of the two populations of fossil microatolls.

Figure S10 (next page). Cross section and growth history plot of the hat-shaped microatoll NPK10-A2 from North Pukarayat (symbols as in Fig. S5). This coral appears to record two significant uplift events separated by about 40 years of rapid tectonic subsidence. The subsidence rate prior to the first uplift is poorly constrained, but was perhaps slower. Dates on this coral have very large uncertainties. The interval between the two events potentially matches 1613/1658 or 1658/1703 (each 45 years). The earlier pair is consistent with all the U-Th ages; however, a large uplift in 1613 is unlikely at this site because neighboring sites had little or no uplift at that time. It is possible that this coral was transported by a tsunami (rather than uplifted) in 1613. The growth pattern of the inner part of the coral is potentially consistent with partial overturning. However, our preferred hypothesis is that the two uplifts occurred in 1658 and 1703, which is inconsistent with only one of the U-Th ages.

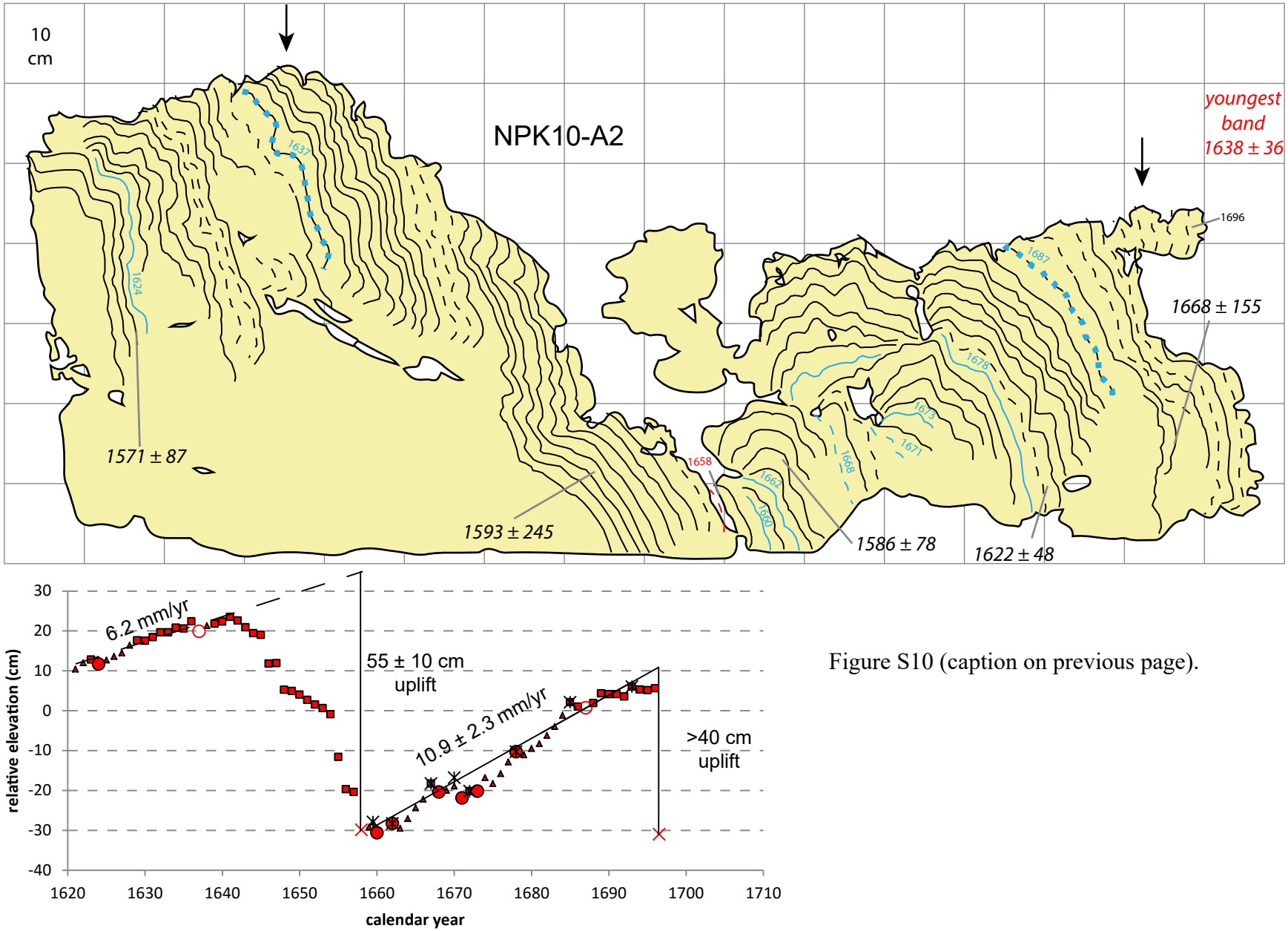

Figure S10 (caption on previous page).

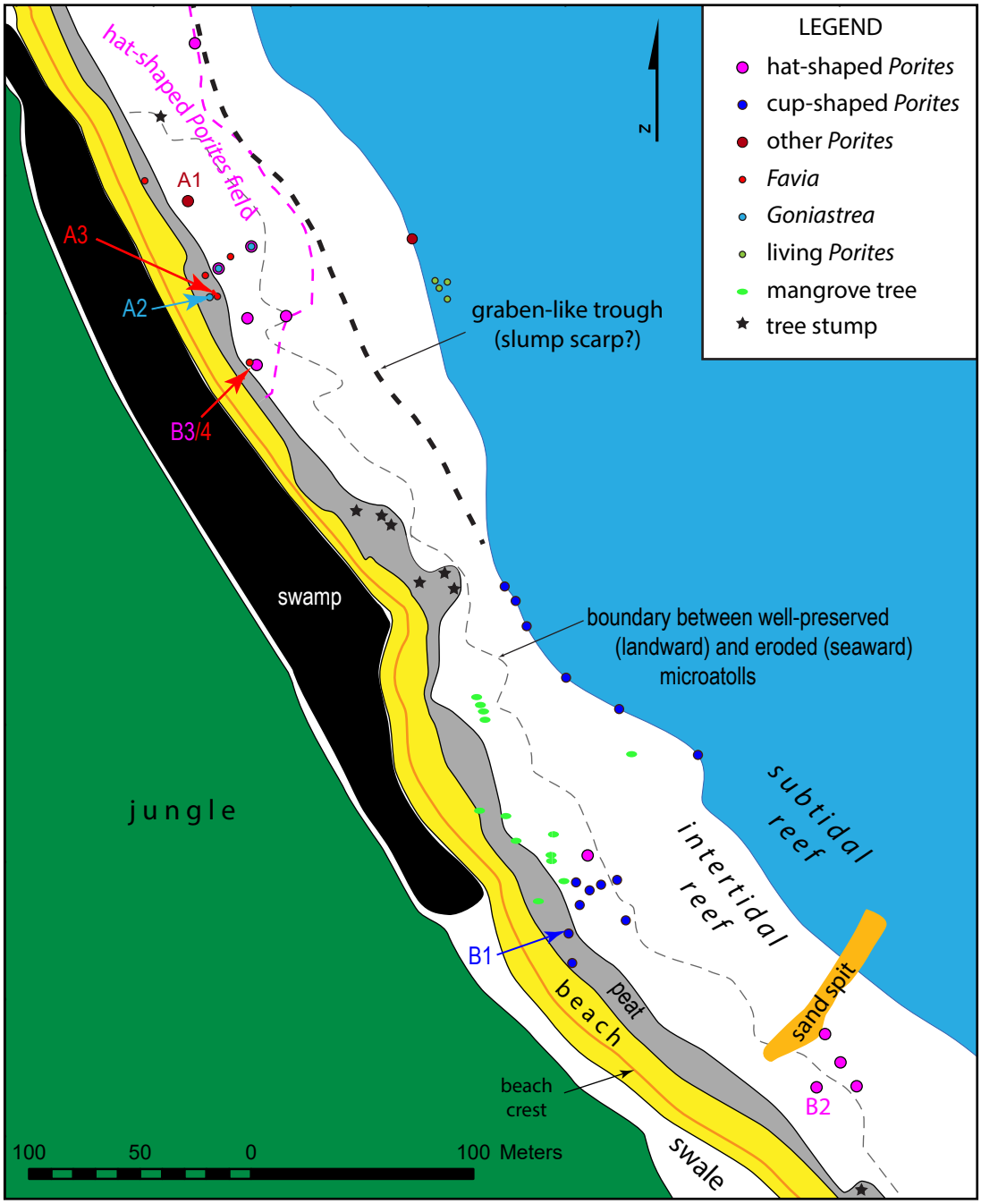

Figure S11. Map of Pasapuat on the northeast coast of North Pagai. A peat layer and embedded jungle tree stumps are evidence of a past coseismic uplift which raised the coral platform above the intertidal zone, and subsequent interseismic subsidence. The peat likely originally extended to the boundary between well-preserved and eroded microatolls, protecting the landward corals from erosion. Microatoll A1 and others of its generation died due to coseismic uplift in ~1390 (see *Philibosian et al.* [2012]). A2 and A3, which were directly covered by the peat, died due to uplift during the 1833 earthquake [*Philibosian et al.* 2014]. All other microatolls died during the 17th century.

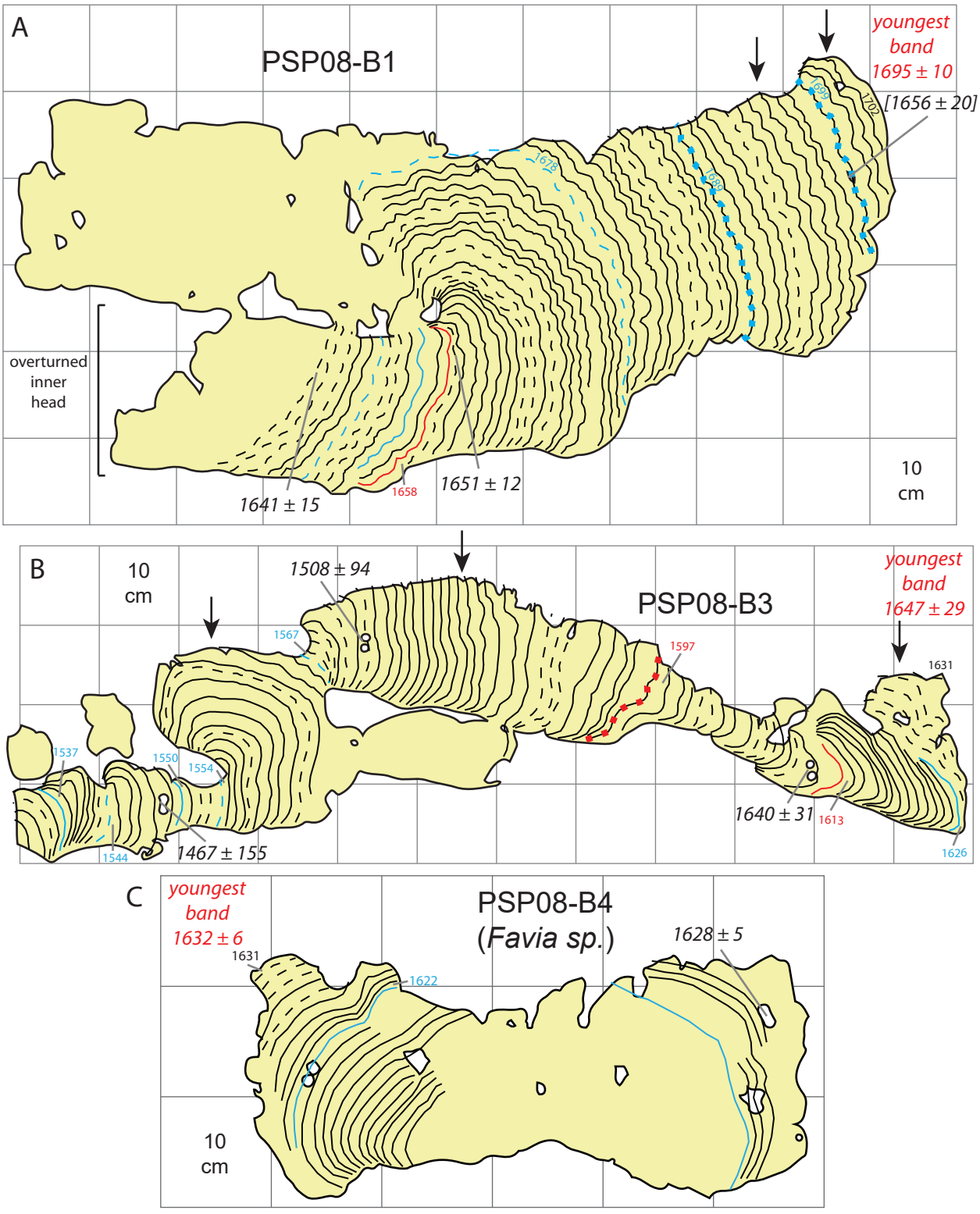

Figure S12. Cross sections of PSP08-B1, B3, and B4 from Pasapuat (symbols as in Fig. S5). We exclude the 1656 ± 20 date on B1 as it is inconsistent with the other two dates. The small Favid B4 was embedded in the outer perimeter of B3 and presumably grew contemporaneously.

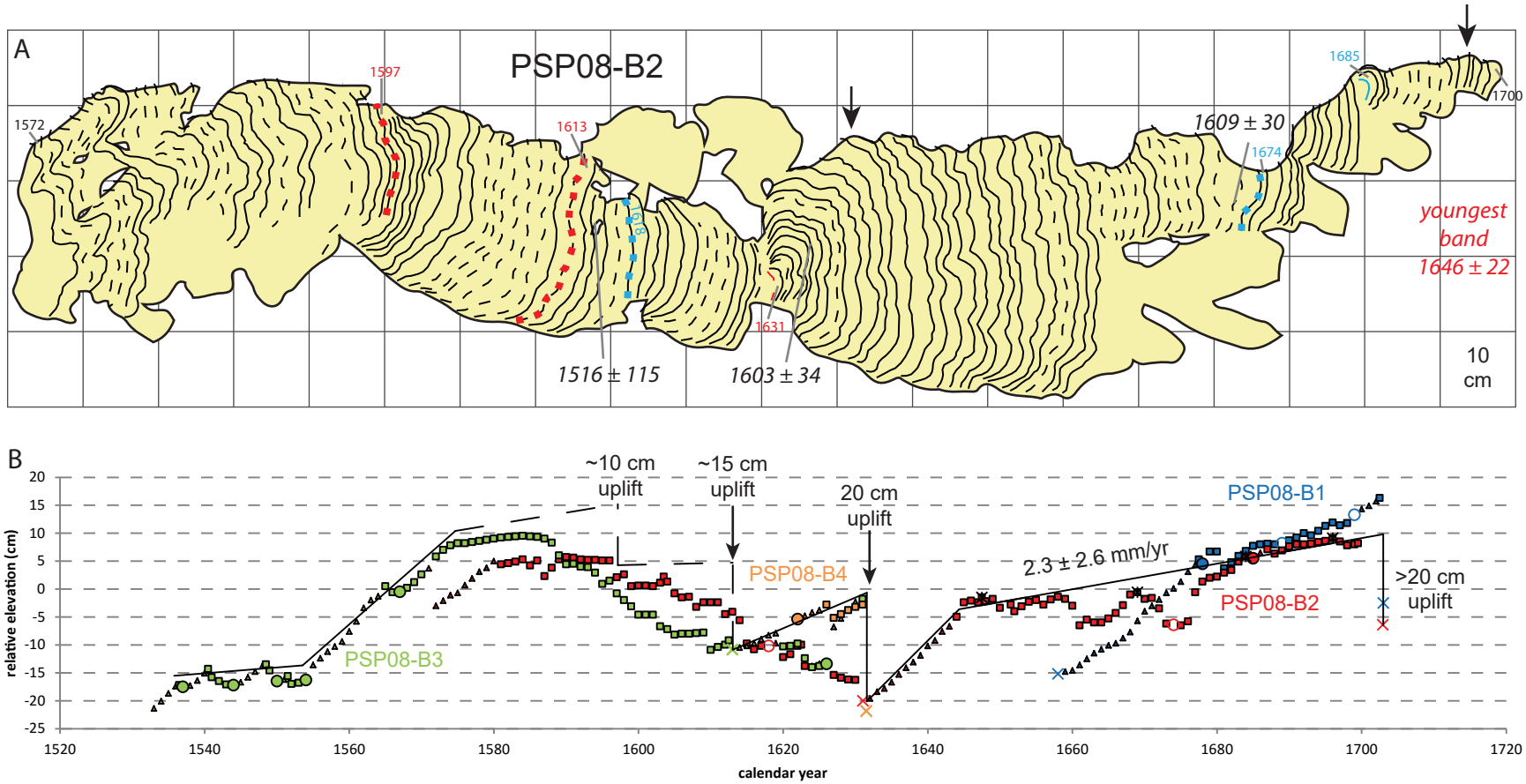

Figure S13. Symbols as in Fig. S5.
A) Cross section of microatoll PSP08-B2 from Pasapuat. The ~35-year period of emergence likely coincides with the similar period recorded by B3, though this interpretation is in conflict with one of the three dates (1609 ± 30).
B) Growth histories of all microatolls from Pasapuat, temporally aligned to match morphologies. The complete record comprises a period of stability in the mid-1500s followed by rapid submergence, emergence from the late 1500s to 1631 (probably including several sudden events), a short period of rapid submergence, slow submergence for the latter half of the 1600s, and finally uplift around 1700.

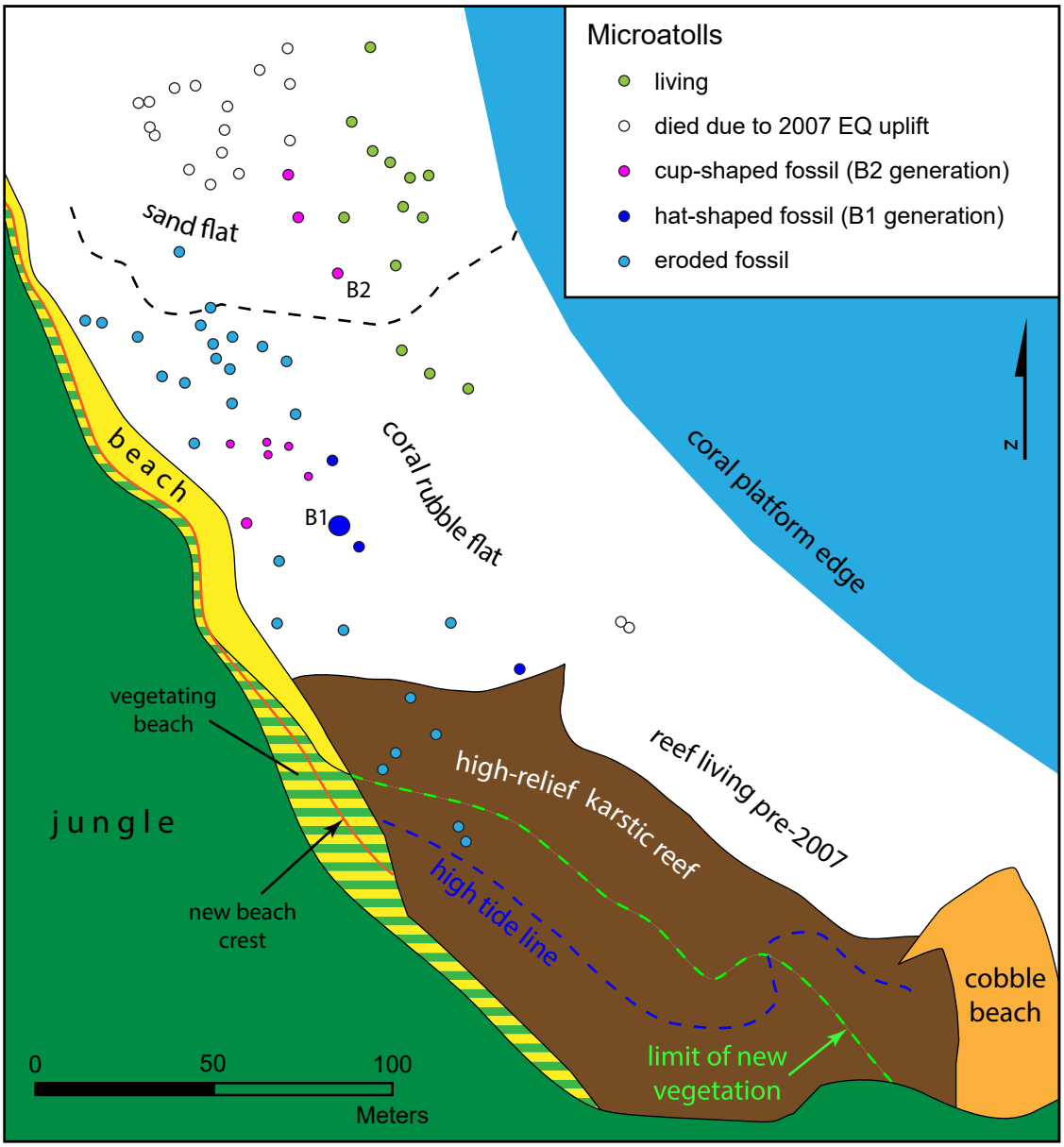

Figure S14. Map of Pecah Belah site B, on a small island in the South Pagai archipelago. Uplift during the 2007 earthquake (68 cm) killed much of the reef at this site and permitted vegetation to establish on the old beach and former intertidal zone. The younger cup-shaped generation of fossil microatolls (B2 group) died due to uplift during the 1833 earthquake [*Philibosian et al.* 2014]. The B1 generation is the same group sampled by *Zachariasen* [1998] as P96L1, later mis-located by *Sieh et al.* [2008] on Taitanopo Island. The B1 group died at the beginning of the 18th century.

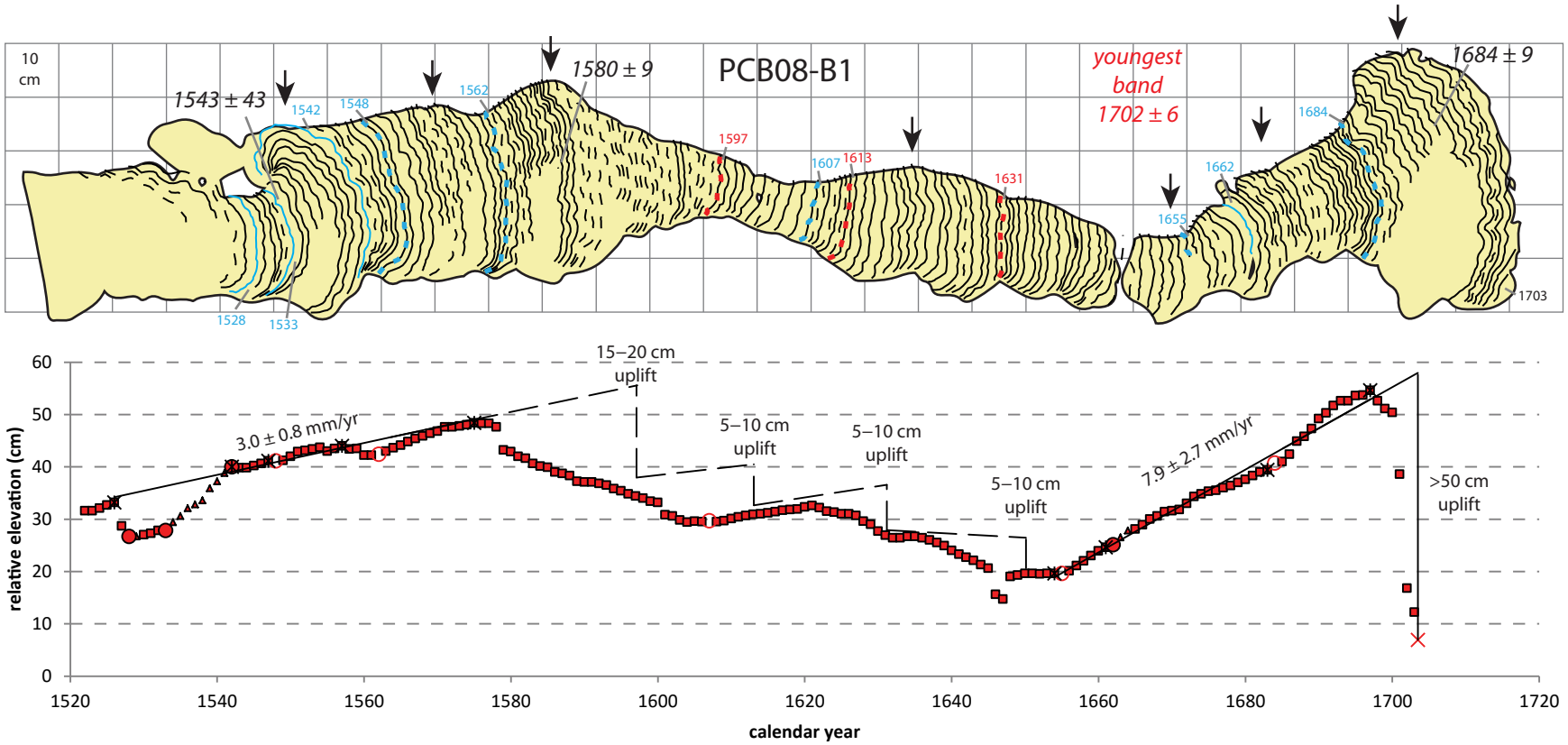

Figure S15. Cross section and growth history of the large hat-shaped microatoll PCB08-B1 from Pecah Belah B, the longest continuous record in our 16th–17th century dataset (symbols as in Fig. S5). The detached outer rim has been restored to its likely original orientation and elevation based on leveling its tilted concentric rings and aligning it with the edge of the inner microatoll. This microatoll clearly documents ~60 years of slow submergence leading up to ~70 years of emergence, followed by ~50 years of more rapid submergence. A final large uplift of at least 50 cm killed the colony. The details of the emergence period have been obliterated by erosion, so it is unclear exactly when and how much uplift took place (though concentric rings, marked by black arrows, indicate that there were at least two discrete uplifts). The total uplift was at least 30 cm and perhaps as much as 50 cm, depending on how much subsidence occurred between uplift events. We surmise that the bulk of the uplift probably occurred during the same three events (1597, 1613, and 1631) identified elsewhere, but it appears that uplift continued until ~1650 at this site.

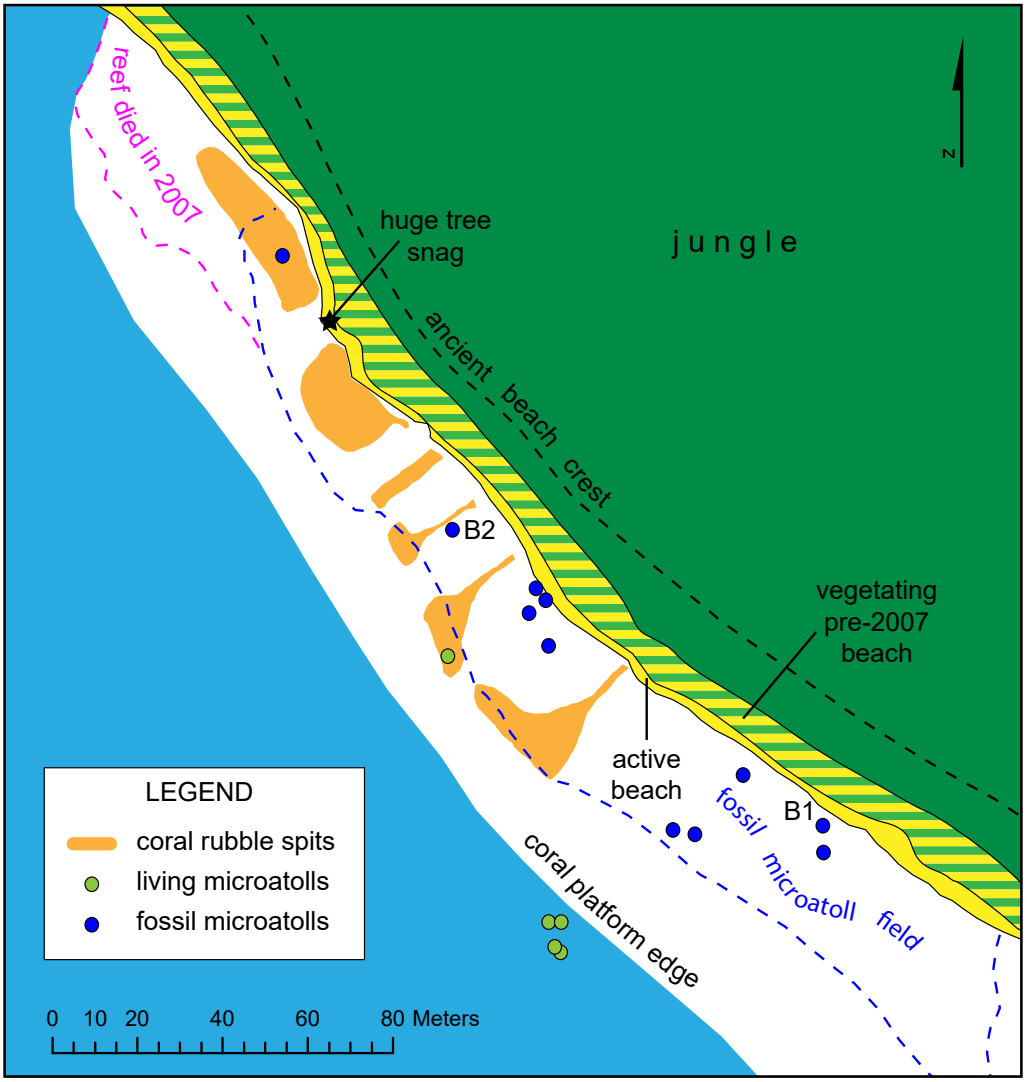

Figure S16. Data from Pulau Kumbang.
A) Map of the site, on a small islet in the South Pagai archipelago. Coseismic uplift in 2007 killed much of the living reef and permitted vegetation growth over most of the beach. A broad swath of cup-shaped fossil microatolls died (presumably also due to coseismic uplift) in about 1700. An ancient beach crest likely corresponds to this fossil population. This fossil population is the same group sampled by *Zachariasen* [1998] as P96M1, later mis-located by *Sieh et al.* [2008] on Siatanusa Island. On the southern tip of Pulau Kumbang, 400 m to the southeast of the B1/B2 field, is a population of very small *Goniastrea* microatolls that died due to uplift in 1833, based on the precise date of KBG08-A1. The 1833 population lies about 30 cm above the c.1700 population.
B) Cross section of KBG10-B1, which records 40 years of moderate interseismic subsidence before its emergence and death.
C) Cross section of KBG10-B2, which has a large date uncertainty but we infer died at the same time as B1. Moderate interseismic subsidence clearly persisted for 80 years prior to the uplift.
D) Growth history of B1 and B2, with a well-resolved subsidence rate derived from the less eroded parts of both corals. No more than a few cm of uplift occurred in 1631.

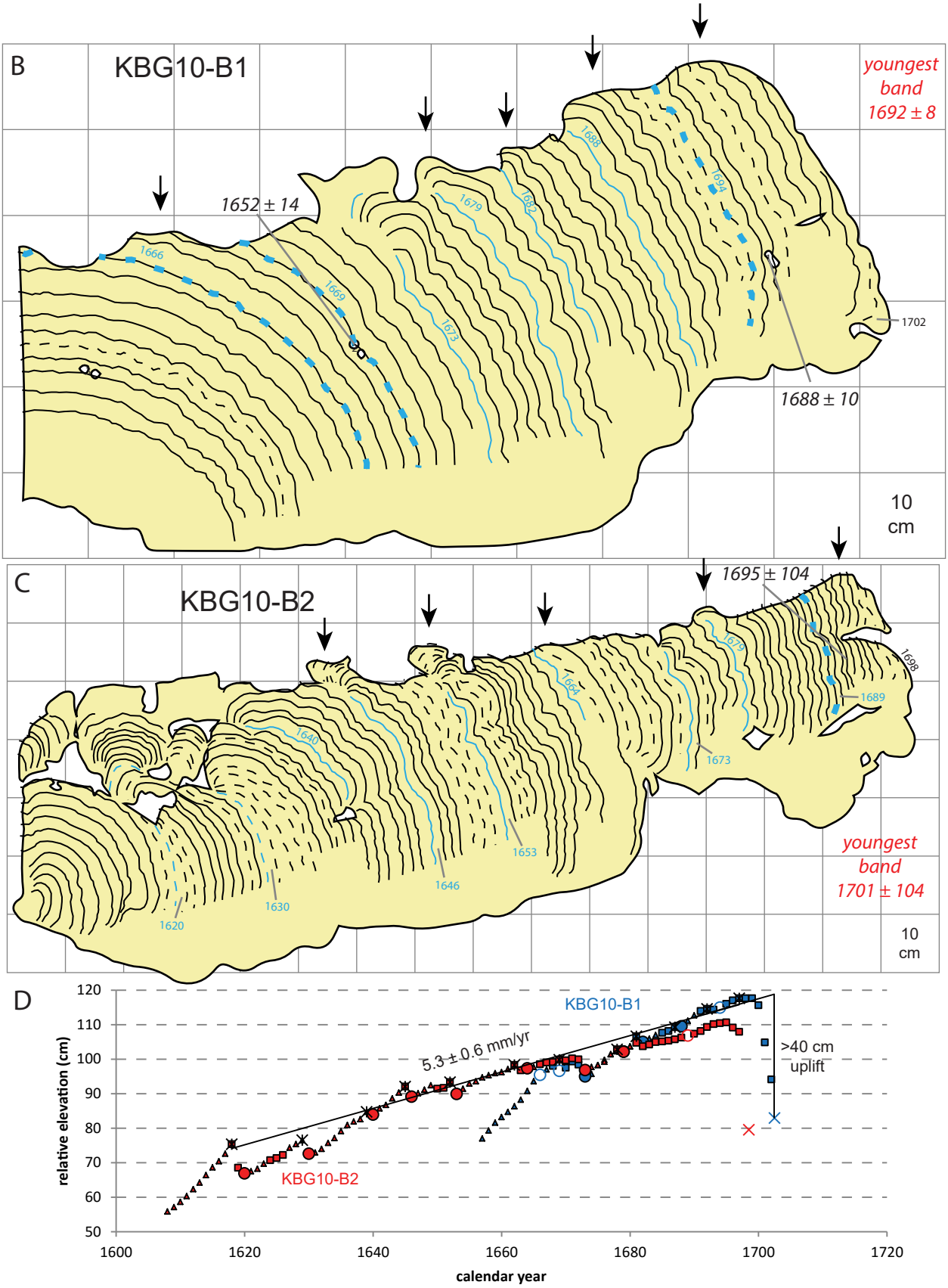

Figure S16 (continued). Symbols as in Fig. S5.

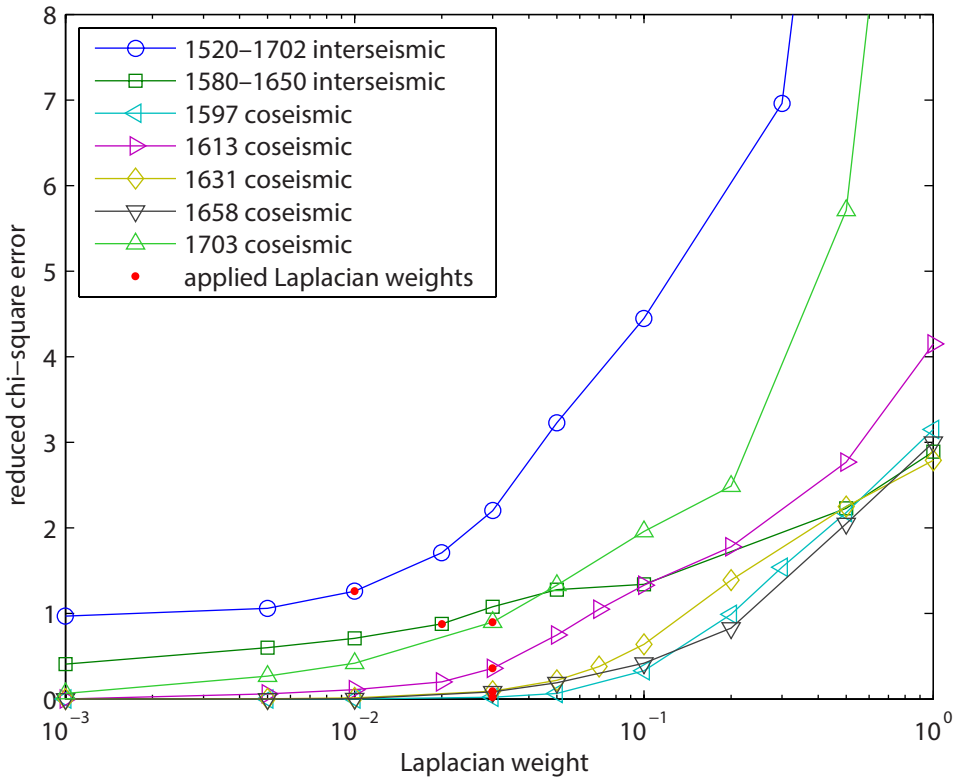

Figure S17. Reduced chi-square error vs. Laplacian penalty (smoothing factor) for models. The Laplacian weights were placed at the point on the curve where the misfit begins to rapidly increase. For ease of comparison, all interseismic models use 0.02, chosen based on the 1580–1650 interval which can tolerate the least smoothing. Similarly, all coseismic models use 0.03, based on the 1613 and 1703 models.

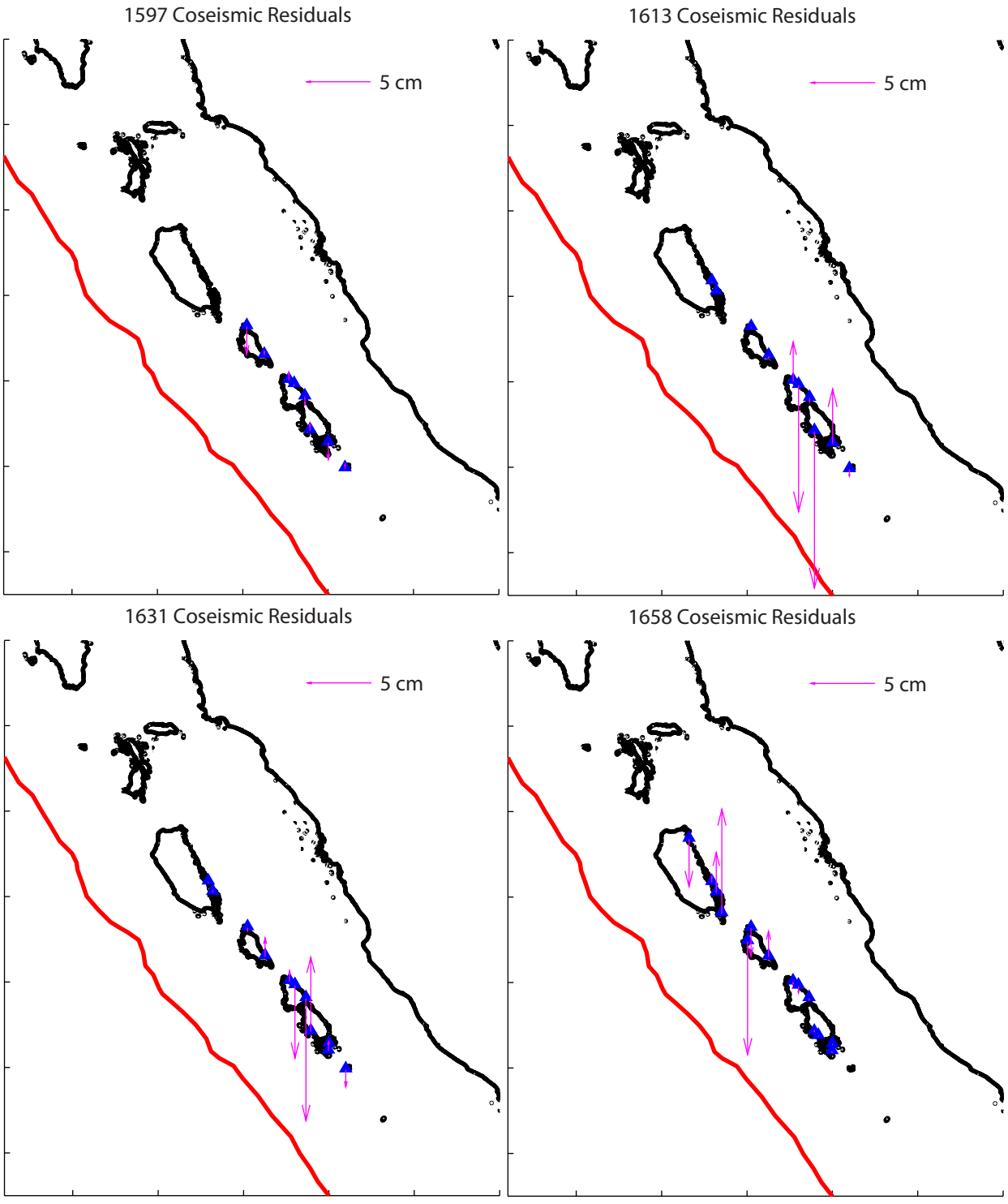

Figure S18. Residuals for the 1597–1658 coseismic models.

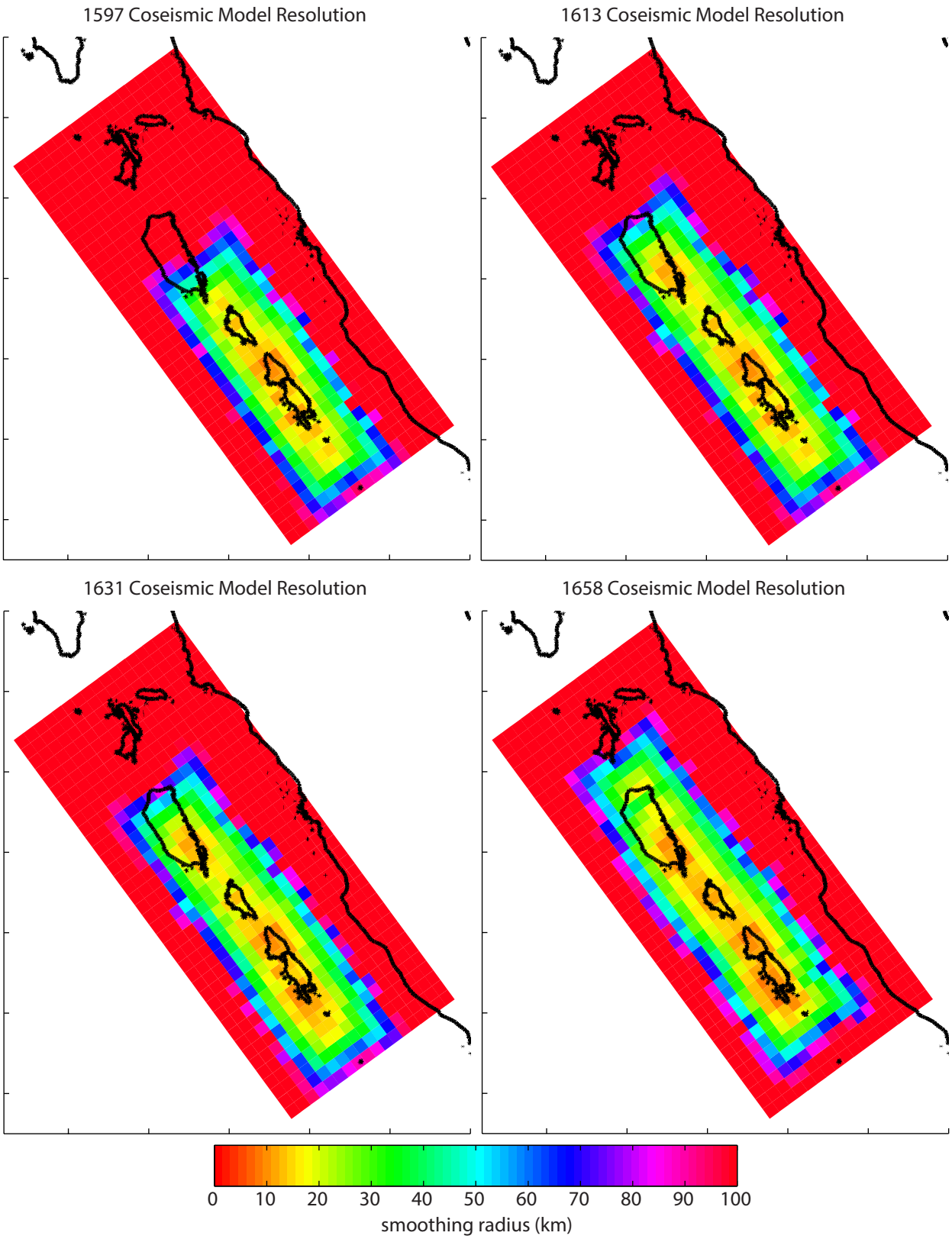

Figure S19. Resolution of the 1597–1658 coseismic models. The slip on each fault element is smoothed with all other elements within its smoothing radius.

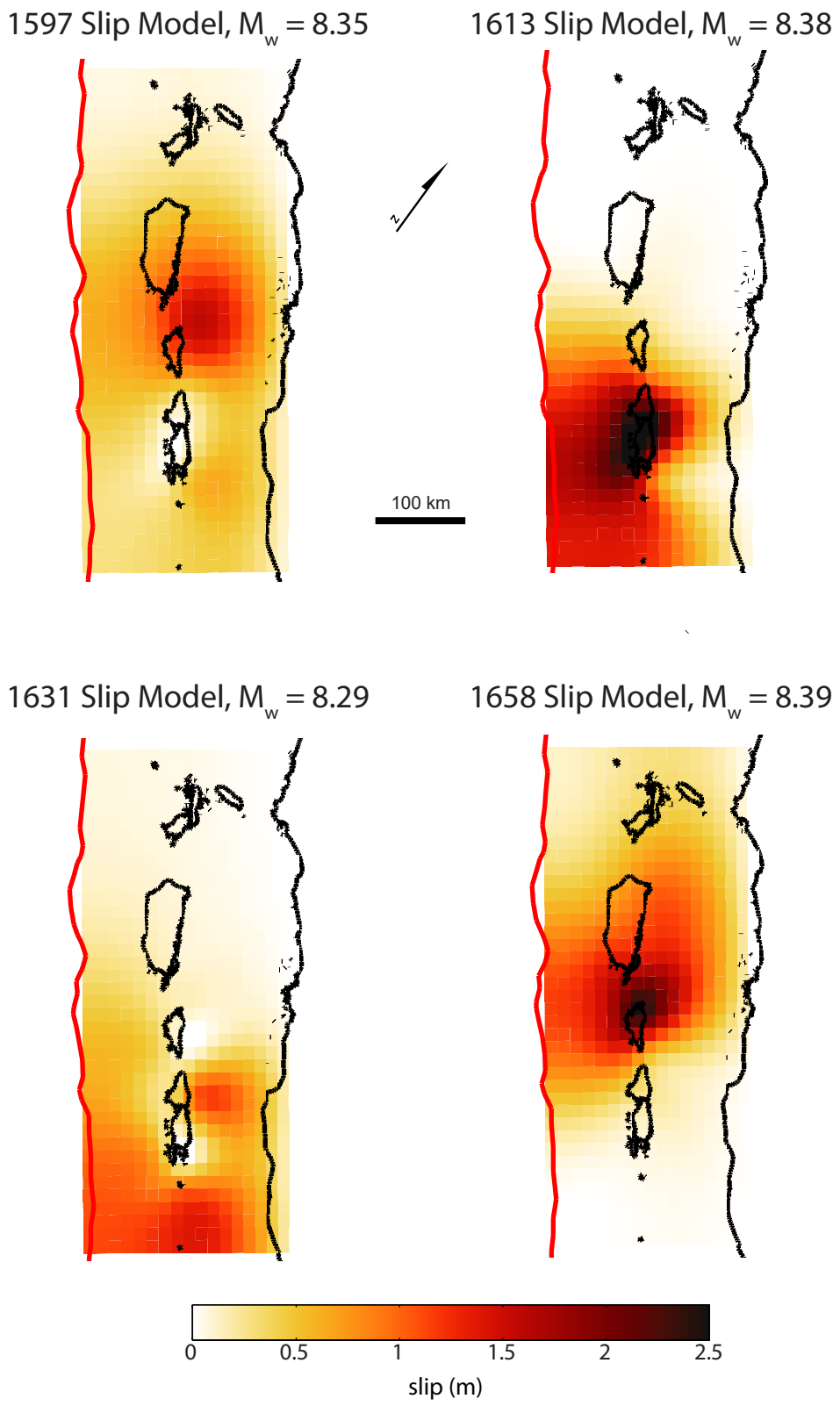

Figure S20. Alternate slip models for the 1597–1658 events with slip permitted to extend to the upper edge of the megathrust beneath the trench.

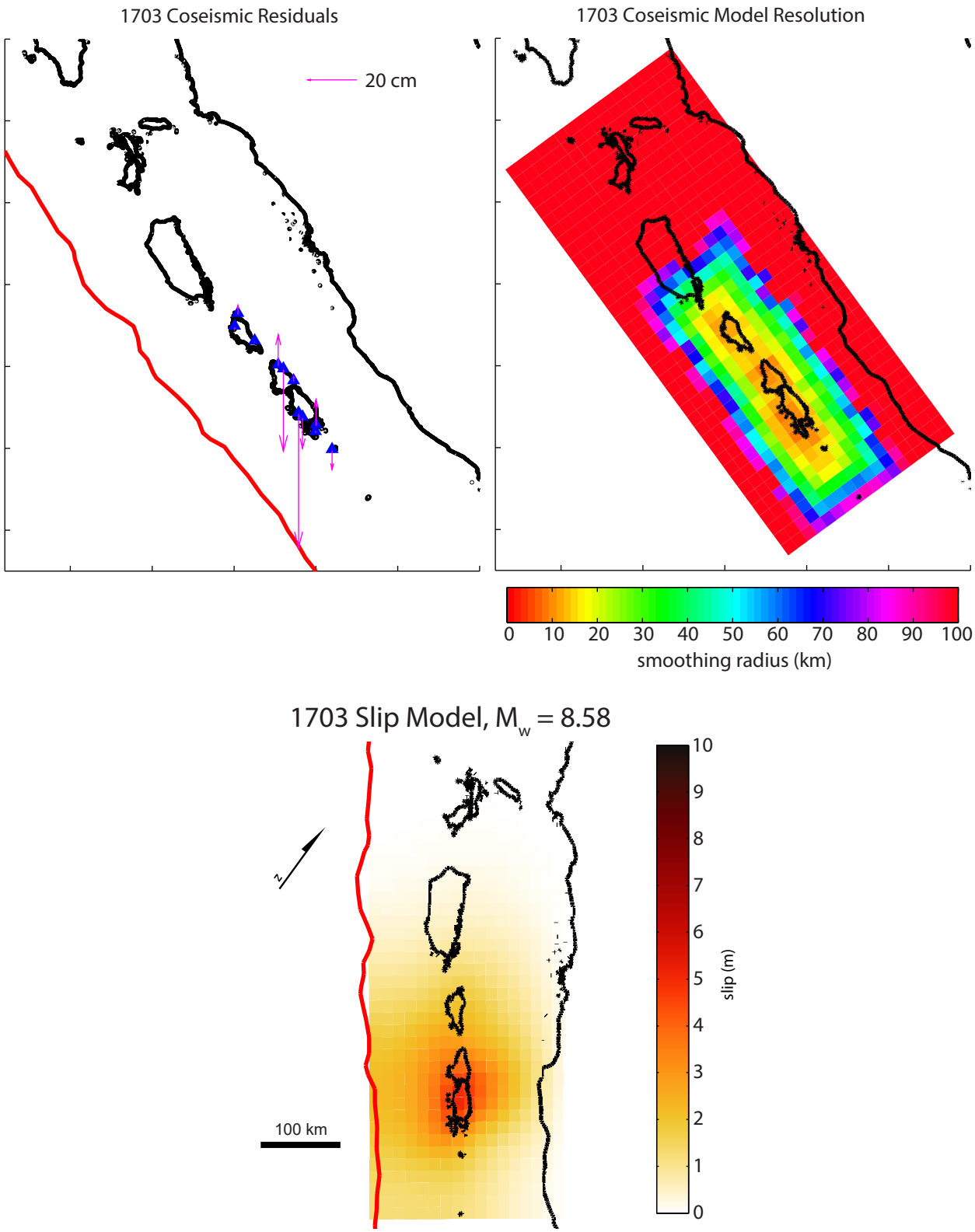

Figure S21. Residuals, resolution, and alternate model allowing slip along the upper edge of the megathrust for the 1703 event. Residuals are much larger than for the other four events, but measurement uncertainties are also much larger (see Table 1).

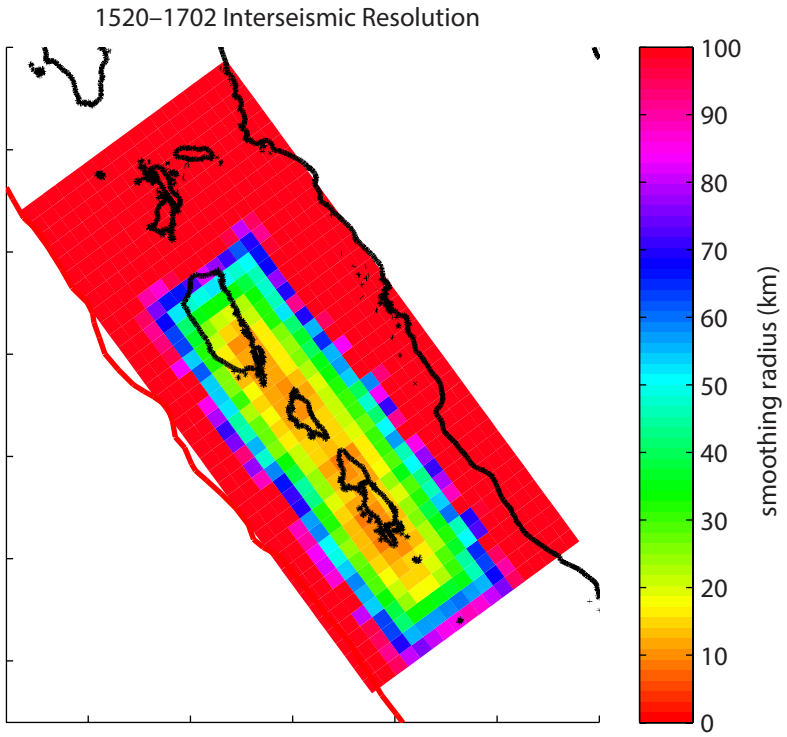

Figure S22. Resolution for interseismic models.

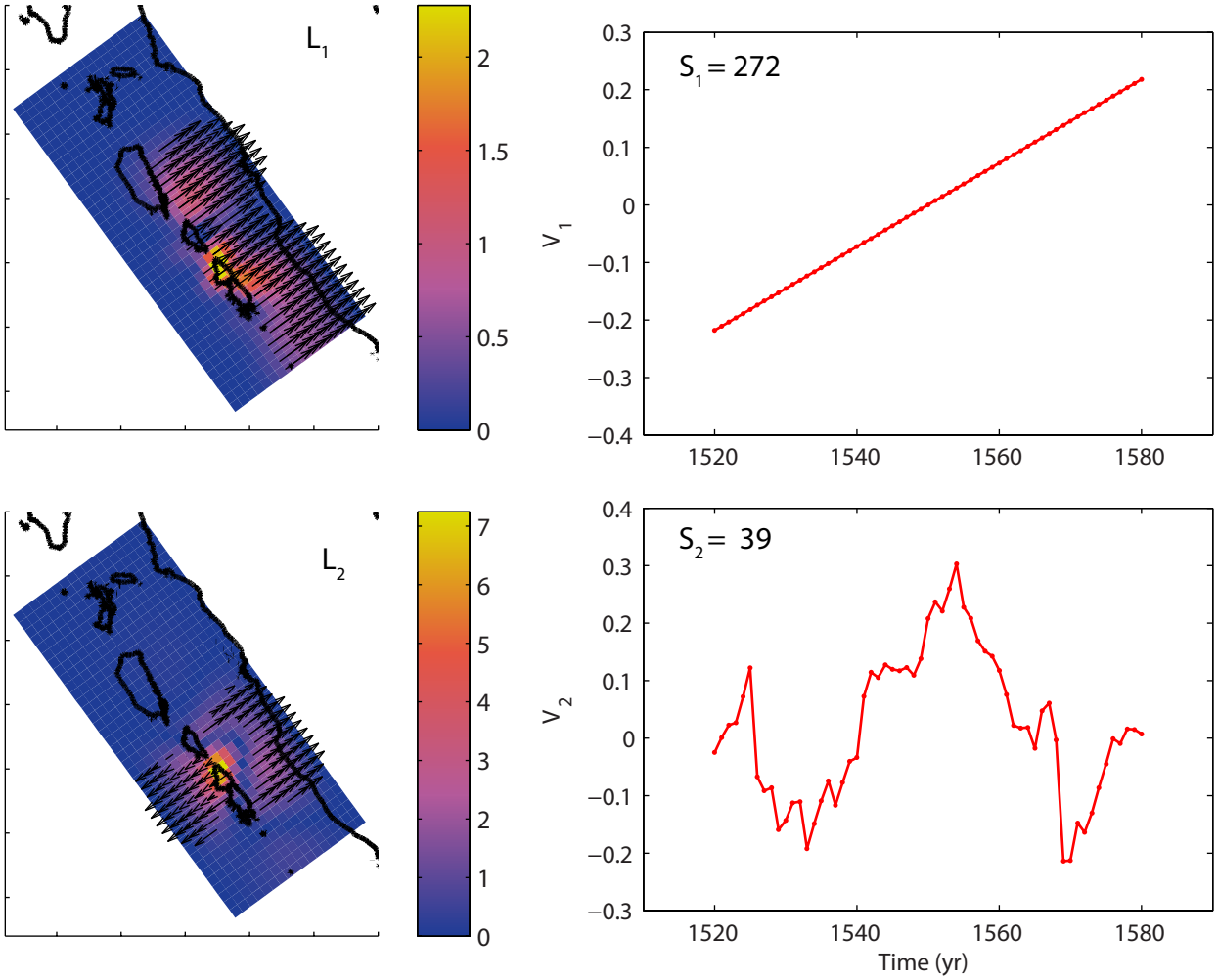

Figure S23. Spatial (L) and temporal (V) eigenvectors and eigenvalues (S) for the 1520–1580 interseismic model.

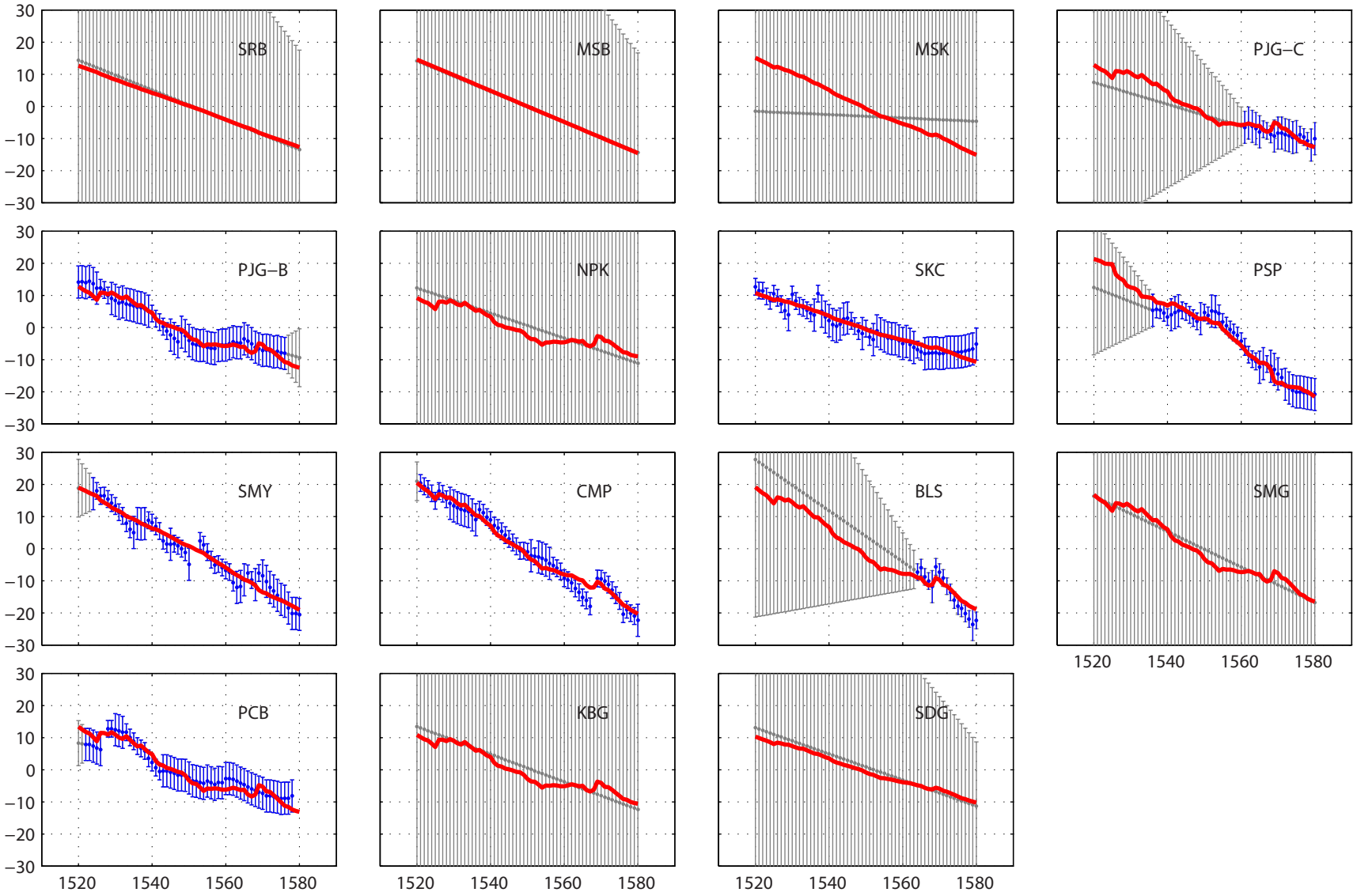

Figure S24. Coral data time series (blue) with synthetic supplementation (gray) and model (red) for interseismic deformation during the 1520–1580 period. Y axes are in cm and X axes are in years.

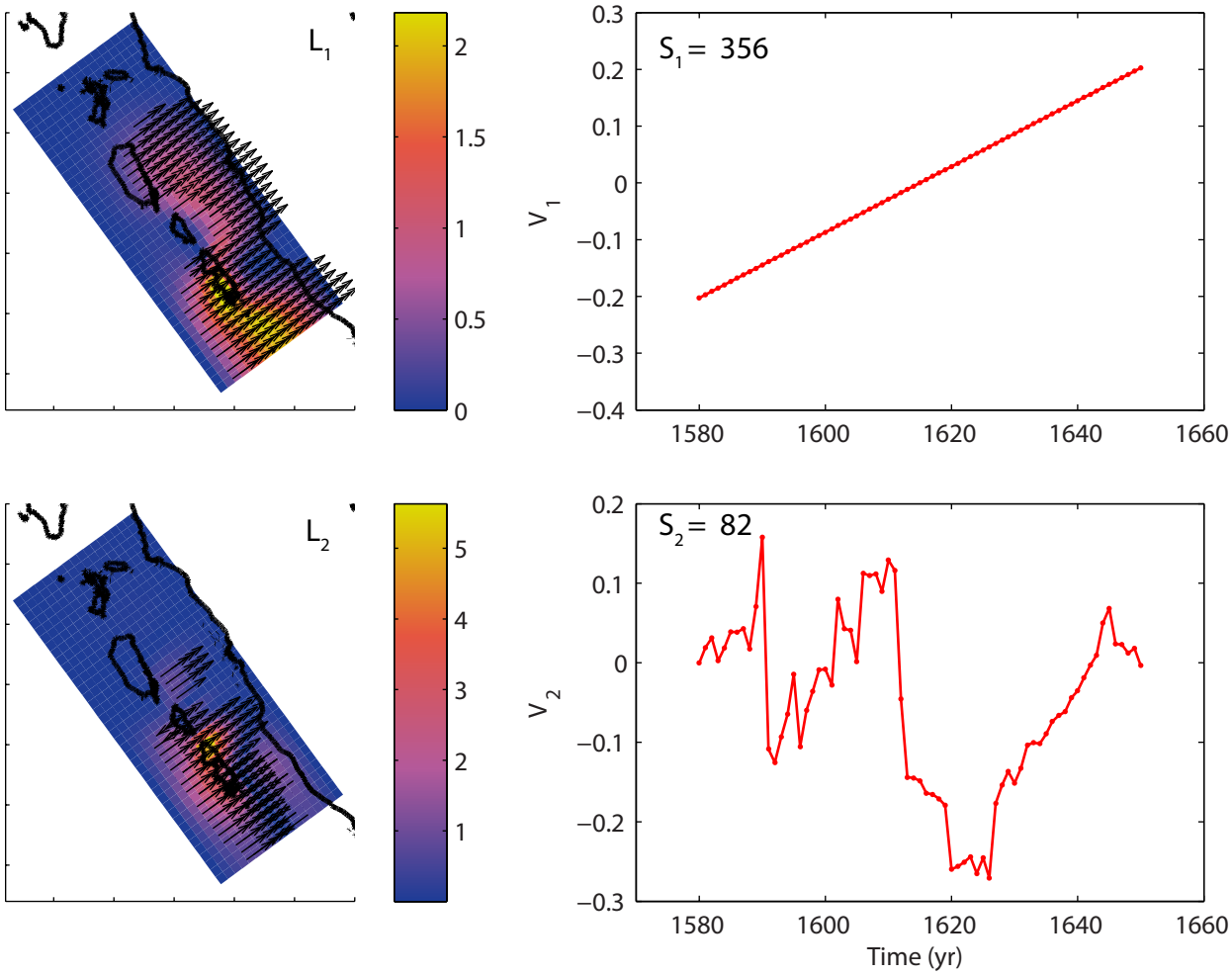

Figure S25. Spatial (L) and temporal (V) eigenvectors and eigenvalues (S) for the 1580–1650 interseismic model.

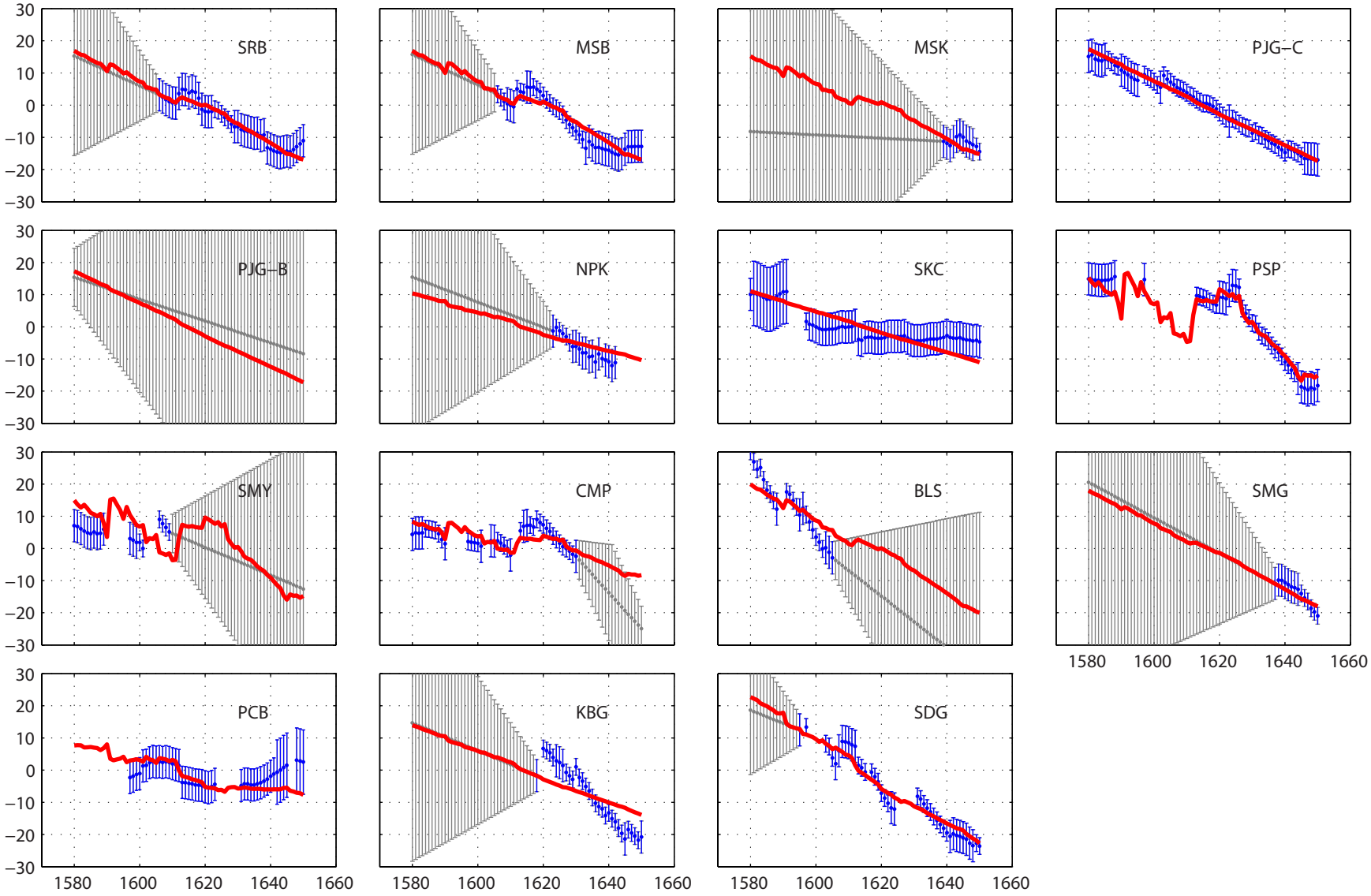

Figure S26. Coral data time series (blue) with synthetic supplementation (gray) and model (red) for interseismic deformation during the 1580–1650 period. Y axes are in cm and X axes are in years.

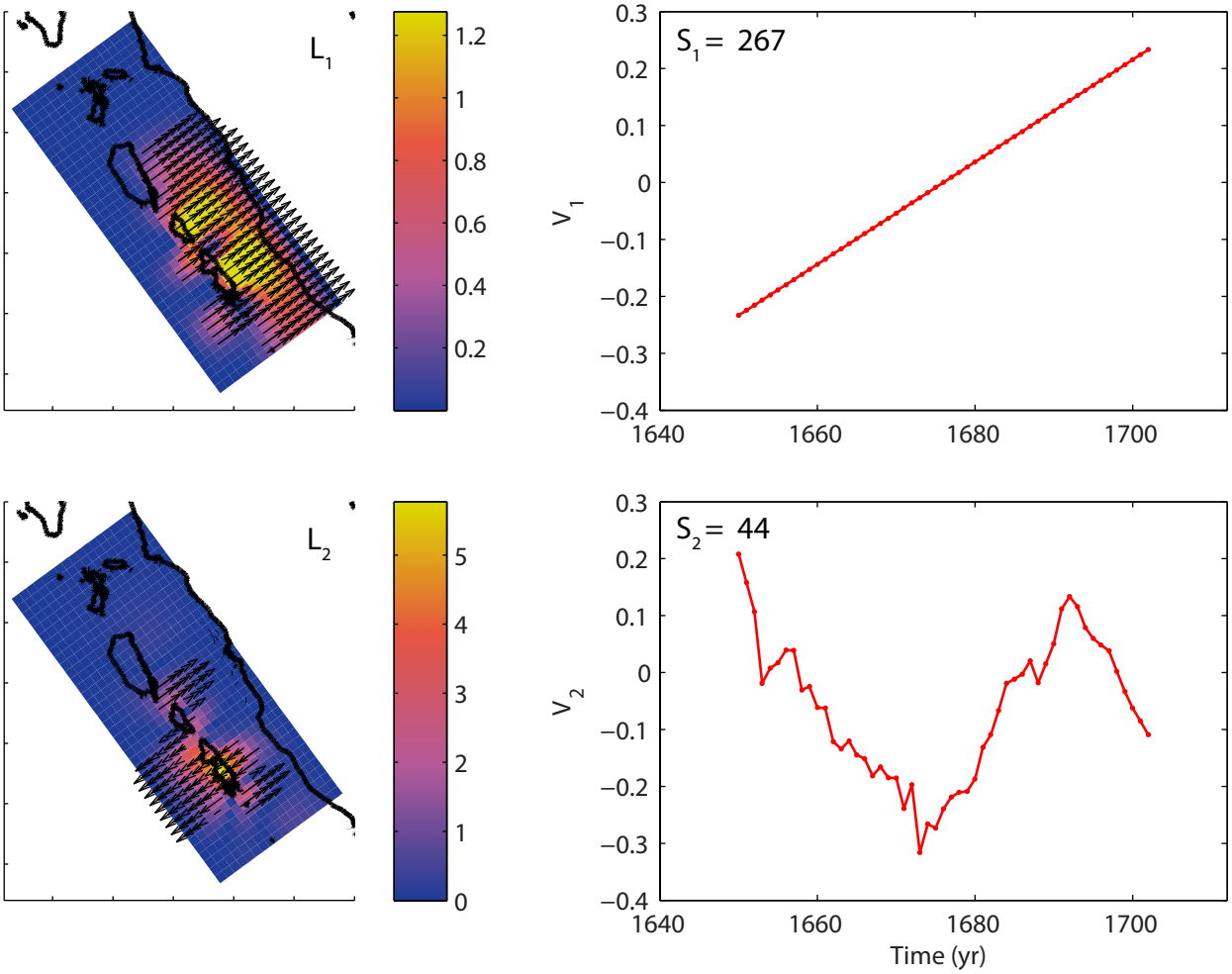

Figure S27. Spatial (L) and temporal (V) eigenvectors and eigenvalues (S) for the 1650–1702 interseismic model.

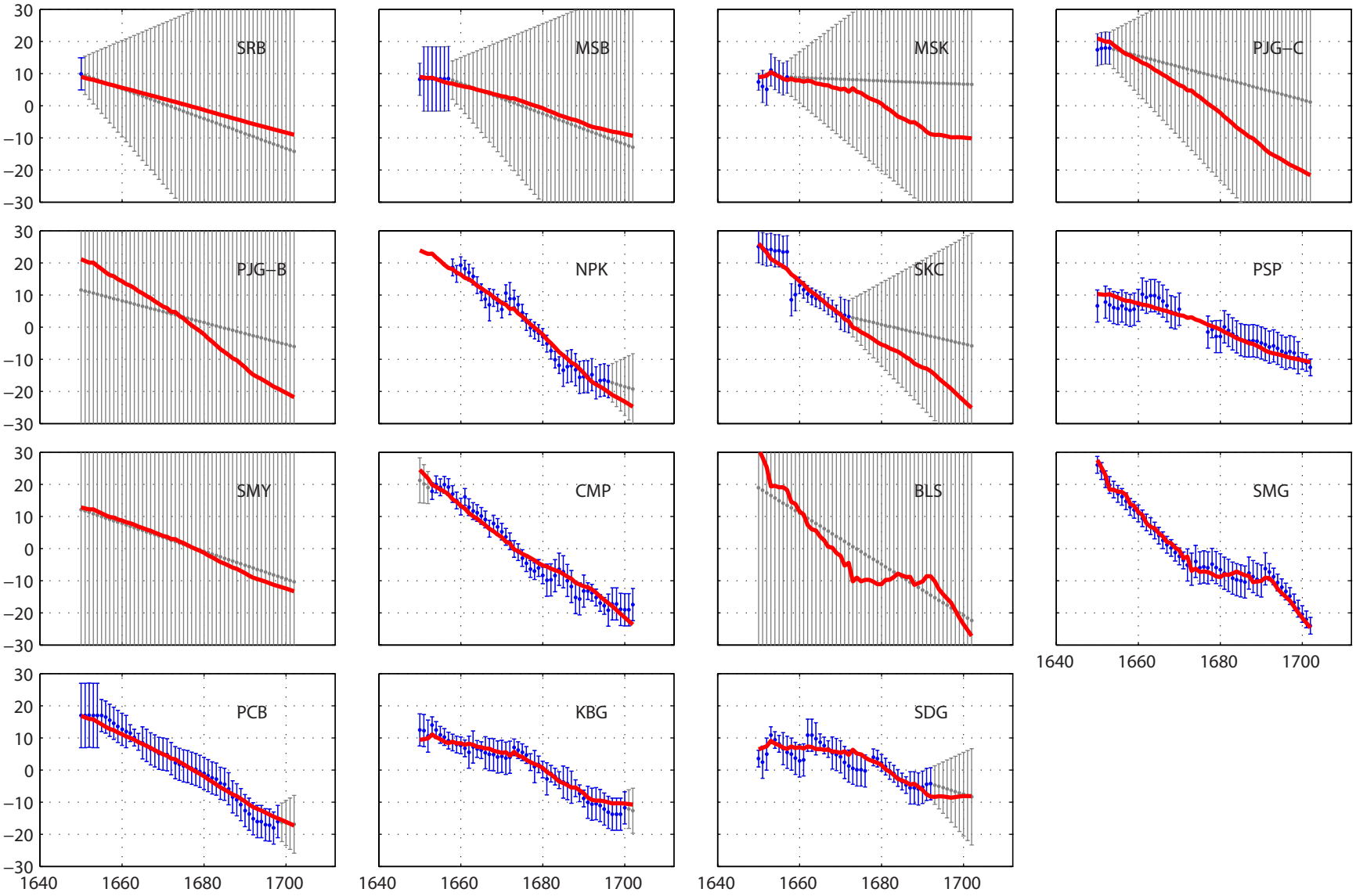

Figure S28. Coral data time series (blue) with synthetic supplementation (gray) and model (red) for interseismic deformation during the 1650–1702 period. Y axes are in cm and X axes are in years.

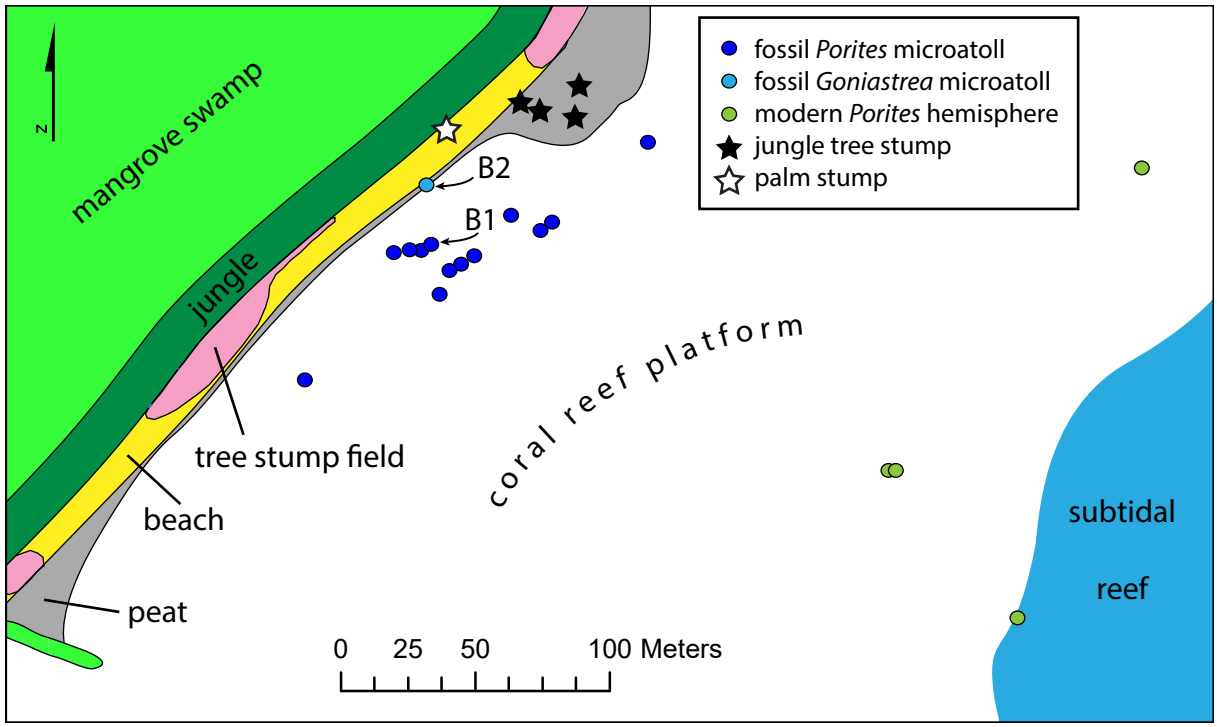

Figure S29. Map of the Silogui B site on the northeast coast of Siberut. The fossil microatoll population died around A.D. 700. The modern reef died almost completely during the 1997–1998 algal bloom, and none of the scarce living corals had yet reached HLS and formed microatolls by the time of our visit in 2010. Therefore, we have only a minimum estimate for modern HLS at this site. As at many other sites, stumps of drowned trees and a peat layer are evidence of past cycles of subsidence and uplift.

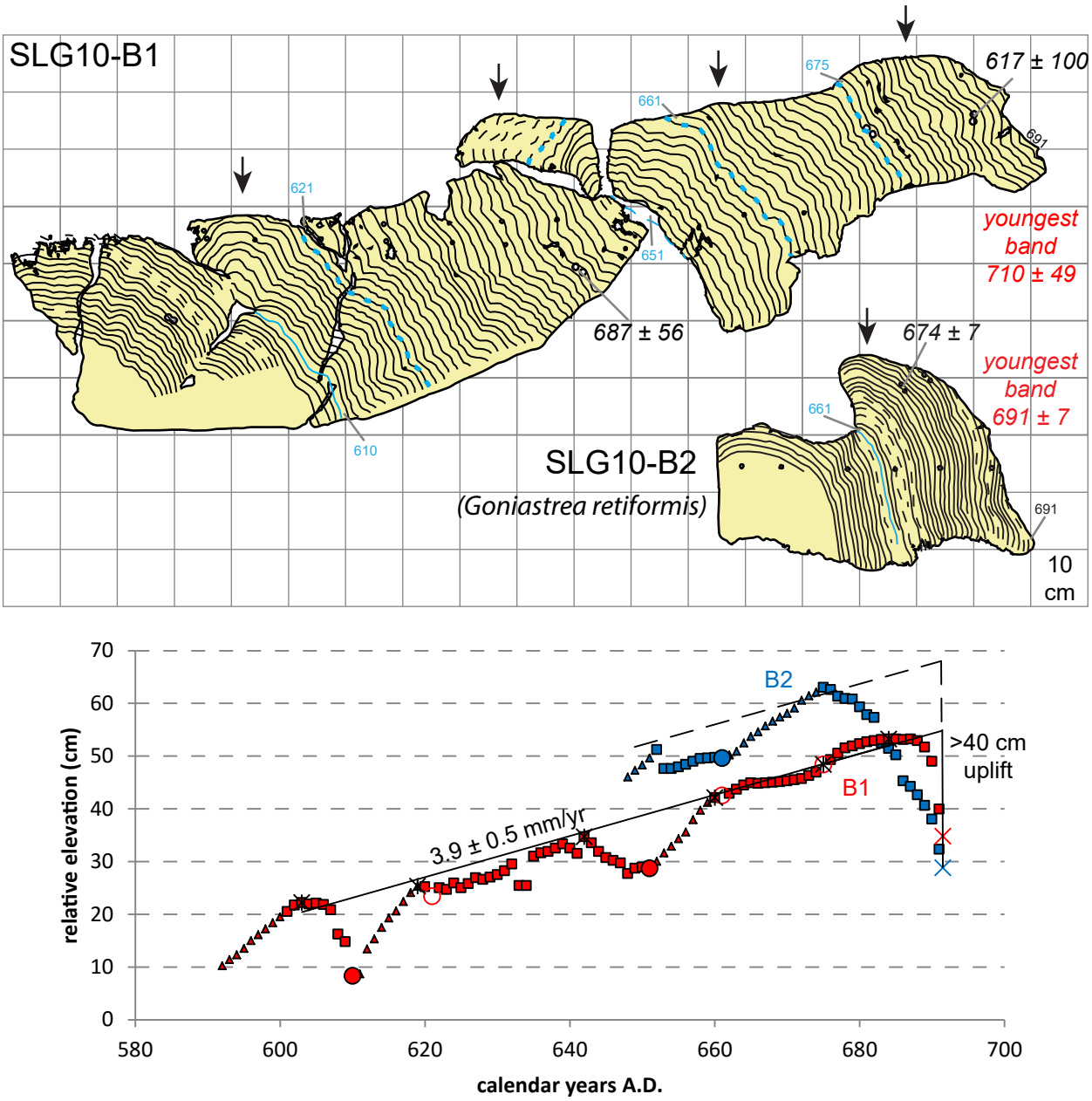

Figure S30. Coral cross sections and growth history plot for the Silogui B site (all symbols as in Fig. S5). B1, a *Porites sp.* colony, recorded a century of submergence at about 4 mm/yr before it was uplifted and died. B2, a *Goniastrea retiformis* colony which grew contemporaneously with the youngest part of B1, provided a much tighter age constraint on the uplift event which killed this population of corals. As is common, the *Goniastrea* HLS was about 10 cm higher than the *Porites* HLS. The vertical thickness of B2 implies uplift of at least 40 cm in the year ~692.

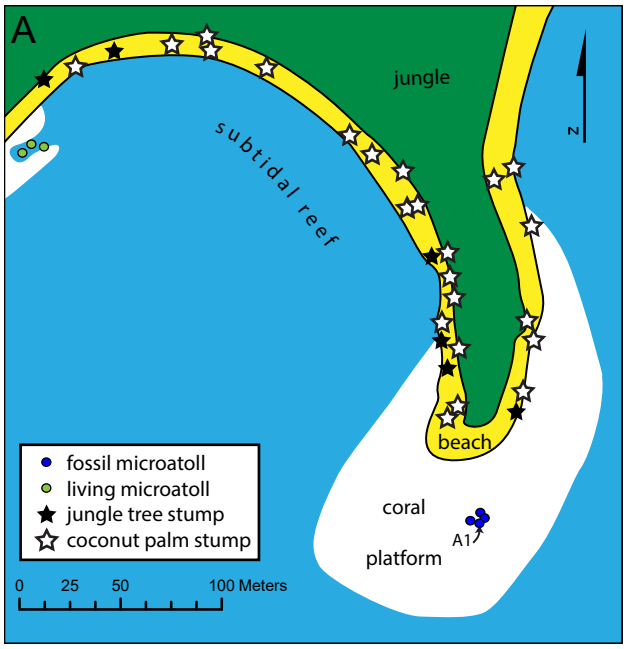

Figure S31. Data from the Teleleu site on southwest Siberut. (A) Map of the site. While there were few living microatolls to be found here, numerous dead trees attest to the ongoing recent interseismic subsidence. (B) Cross section and (C) growth history plot of the microatoll TLU10-A1, which recorded a low rate of subsidence until it was uplifted and died. Band dates are assigned based on comparison with the more precisely dated SSB10-A2 which has a very similar growth history. All symbols as in Fig. S5.

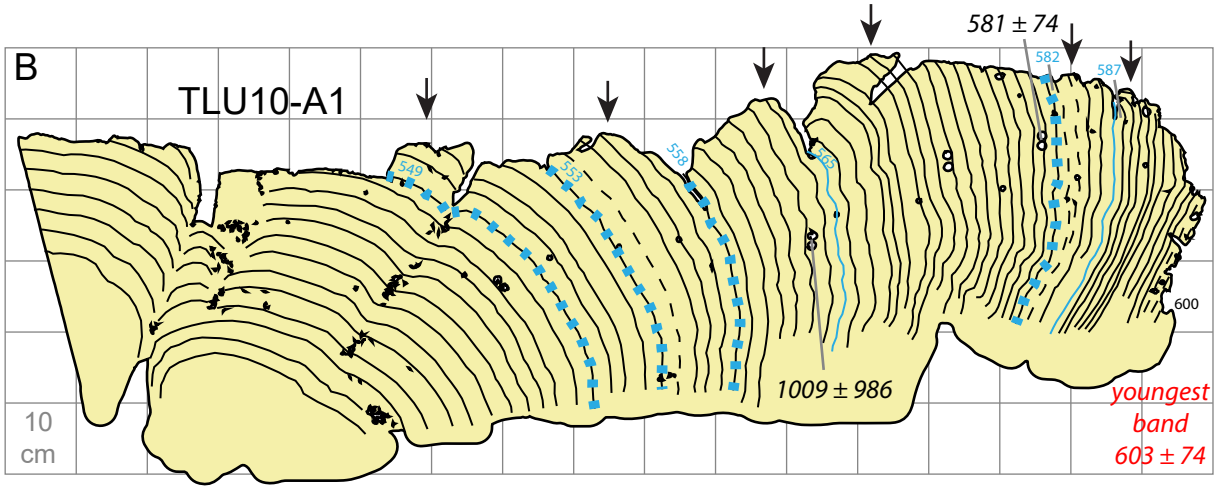

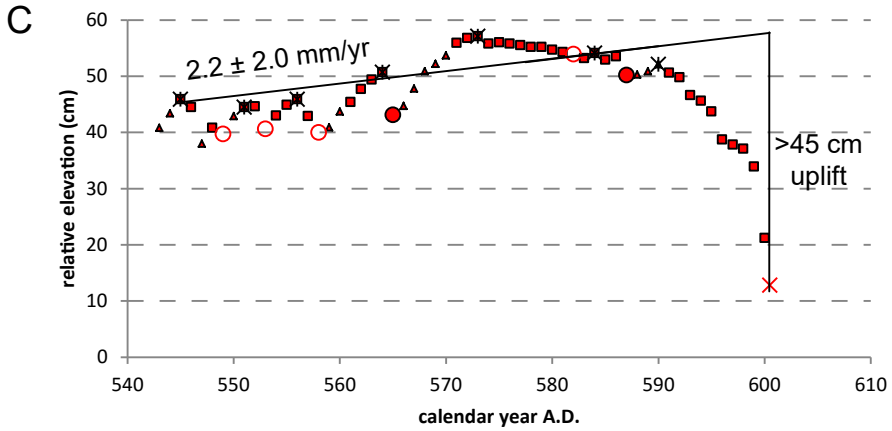

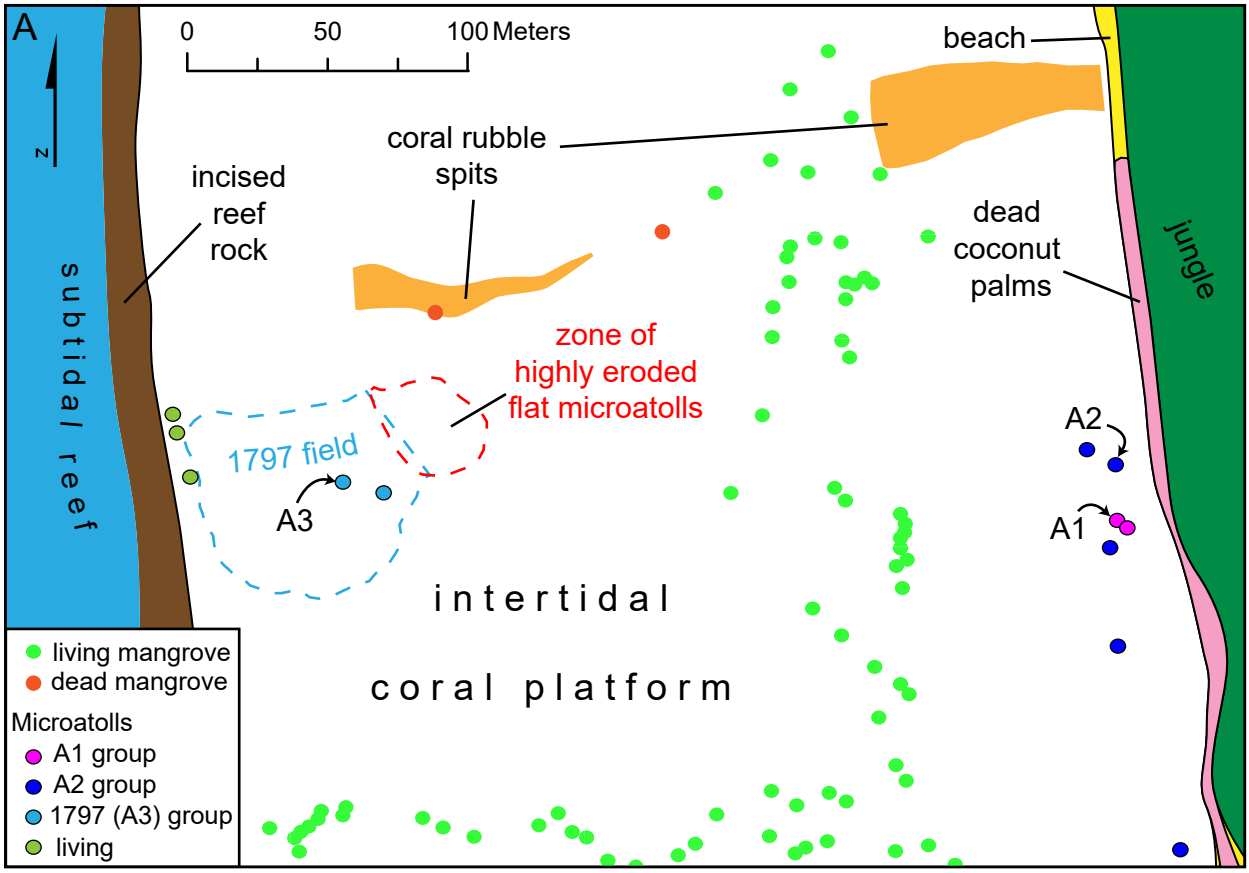

Figure S32. Data from Silabusabeu. (A) Map of the site on the west coast of P. Silabusabeu, an islet near Silabu village on the southwest coast of North Pagai. Few living microatolls could be found at this site, but the band of dead coconut palms attests to the recent interseismic subsidence. The field of fossil microatolls close to the edge of the platform died due to uplift in the 1797 earthquake, as discussed by *Philibosian et al.* [2014]. The two populations near the beach, clearly distinct based on elevation and morphology, both died in the 6th century A.D.

(B) Cross sections and (C) growth history plot of microatolls SSB10-A1 and A2, with all symbols as in Fig. S5. The gray portion of the A1 slab was lost during the thin slicing process and could not be x-rayed. The three U-Th ages obtained for A1 are all mutually inconsistent given the band counting, suggesting that uncertainties are underestimated. We assume the 528 ± 15 date is the most accurate, as the others imply that A1 grew contemporaneously with A2, which is highly improbable given the difference in elevation and morphology. The 528 ± 15 date and the three A2 dates are all consistent within uncertainty with the scenario in which A2 first hit HLS at the time A1 was killed. The composite history indicates a high rate of subsidence for almost 80 years leading up to a pair of moderate uplift events in about A.D. 527 and 530, followed by another 70 years of subsidence at a much lower rate. A final uplift of at least 40 cm killed the A2 population. Assuming this is the same event that killed the Teleleu fossil microatoll population, a few bands must be eroded off the outer surface of A2 and the uplift occurred in ~601. The abrupt change in interseismic subsidence rate at the time of a presumably coseismic uplift event is similar to those observed during the 1600s and after 1797.

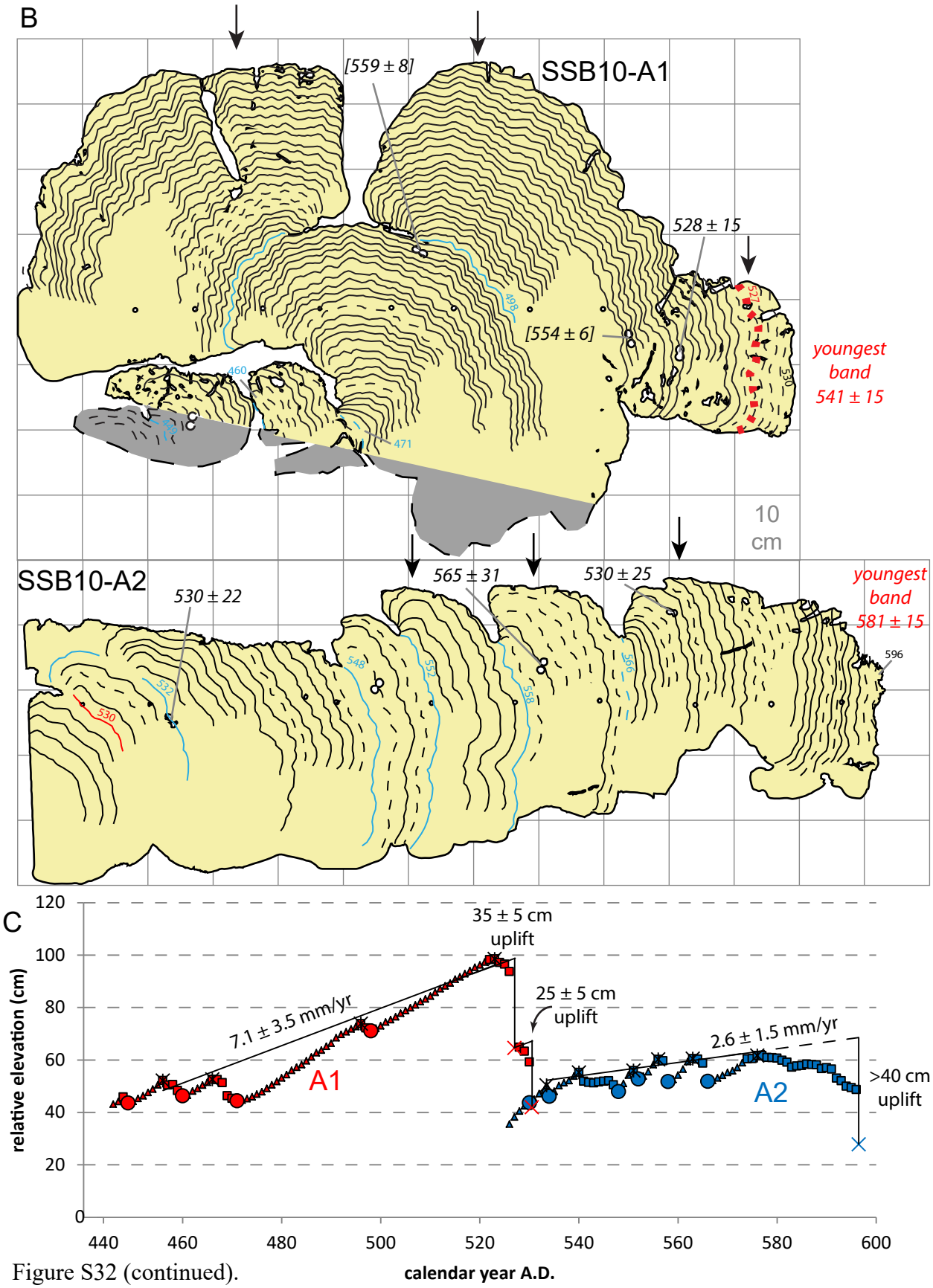

Figure S32 (continued).

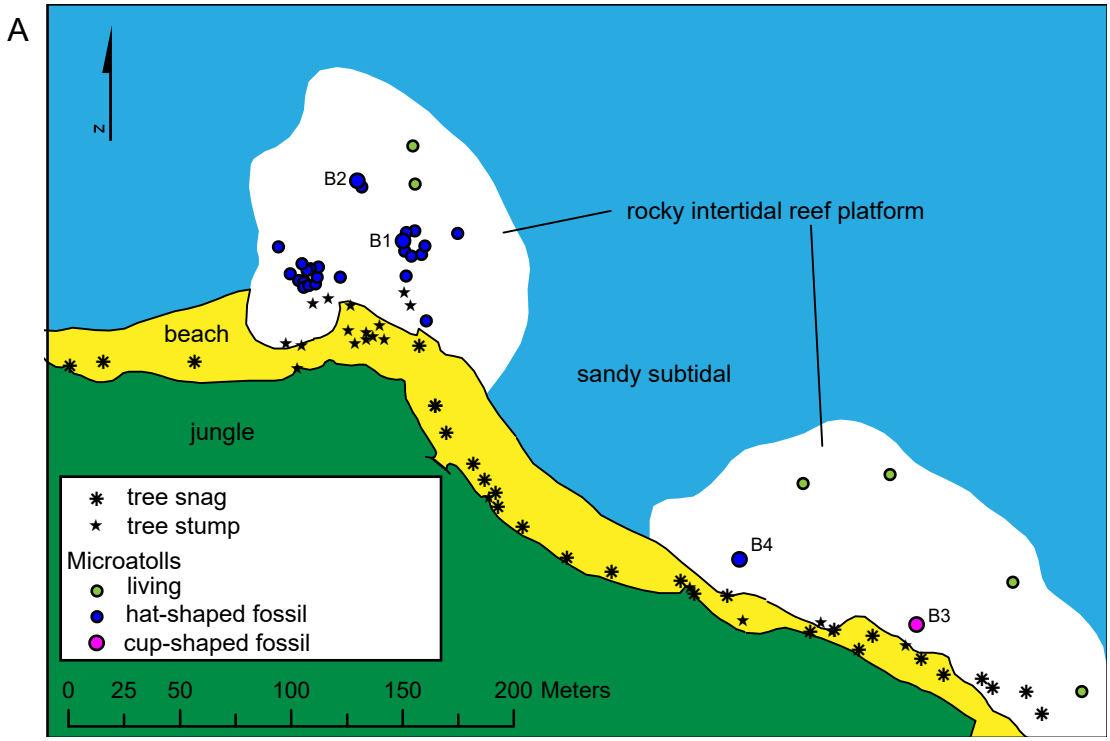

Figure S33. Data from the Basua B site on the east coast of South Pagai.

(A) Map of the site. There is a large field of hat-shaped microatolls of which three were sampled; they appear to represent two or more generations. B3 is much higher elevation and cup-shaped, clearly a distinct generation (only a chiseled sample was collected). Many tree snags and stumps attest to recent interseismic subsidence at this site.

(B) Cross sections of B1, B2, and B4 with symbols as in Fig. S5. B2 has two overlapping slices (the larger one outlined in brown). The B4 slice represents only the outer brim of a larger hat-shaped coral. All three microatolls record at least two large uplifts separated by several decades, but dated samples and growth history differences suggest that B1 does not correlate with B2 and B4. Band years for B2 are assigned based on potential correlation with the more precisely dated B4 (growth histories are more similar to each other than to B1). However, given the very large age uncertainty of B2, it is also possible that it records a third, different pair of uplift events. The interval between first uplift and final uplift/death is 30 years for B1, 40 years for B2, and 45 years for B4. The outer surface of B1 parallels the annual banding, suggesting little erosion and making it unlikely that 10–15 bands have been eroded off. The outer surface of B2 is less pristine and could have 5 bands eroded, and the exact band count of B4 is uncertain, so it is not unreasonable that B2 and B4 could record the same two events.

(C) Growth history plot of the Basua microatolls, with the first tectonic die-down of B1 aligned to the year 794 for comparison with B2 and B4 (though B1 probably actually grew decades earlier).

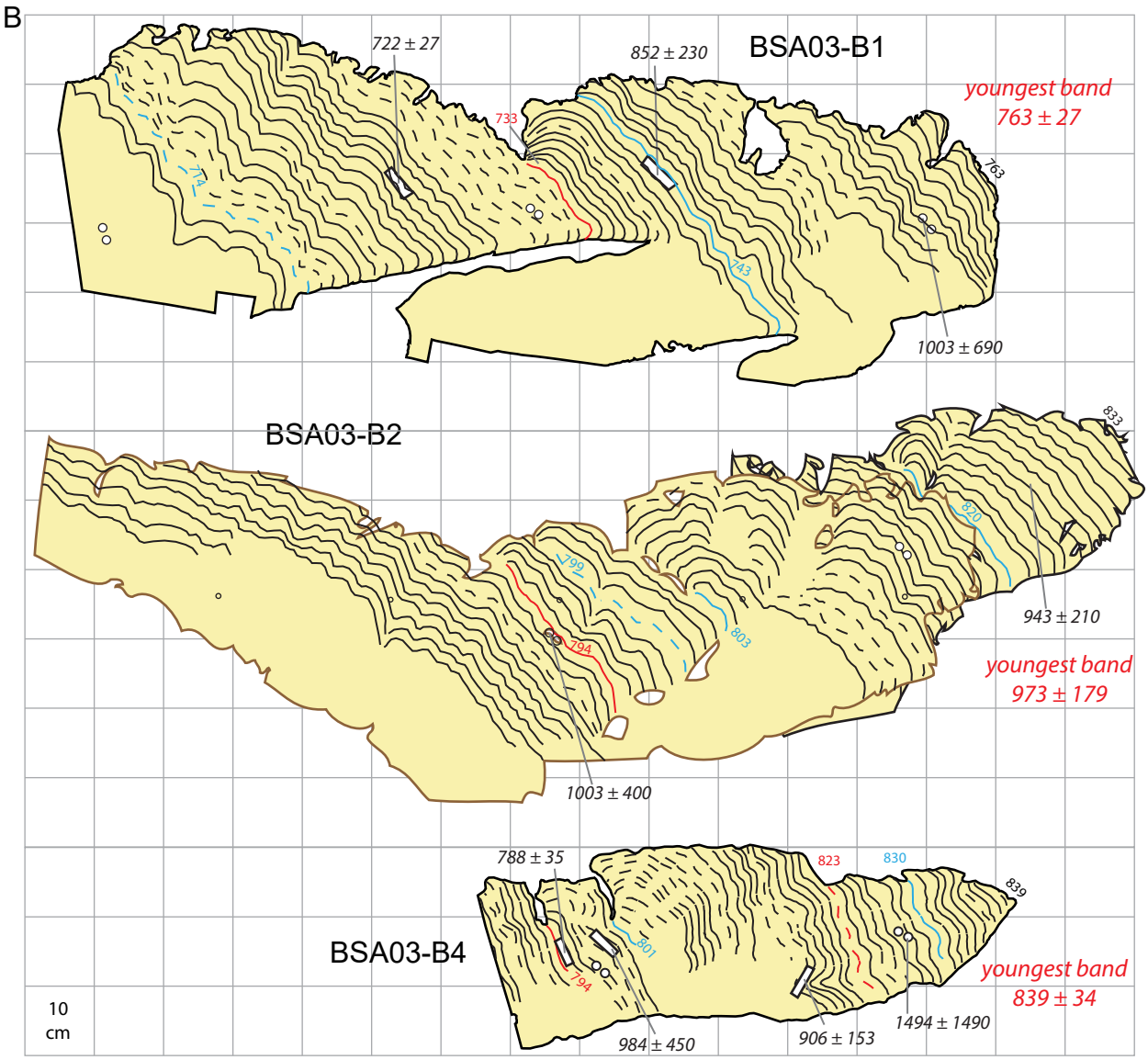

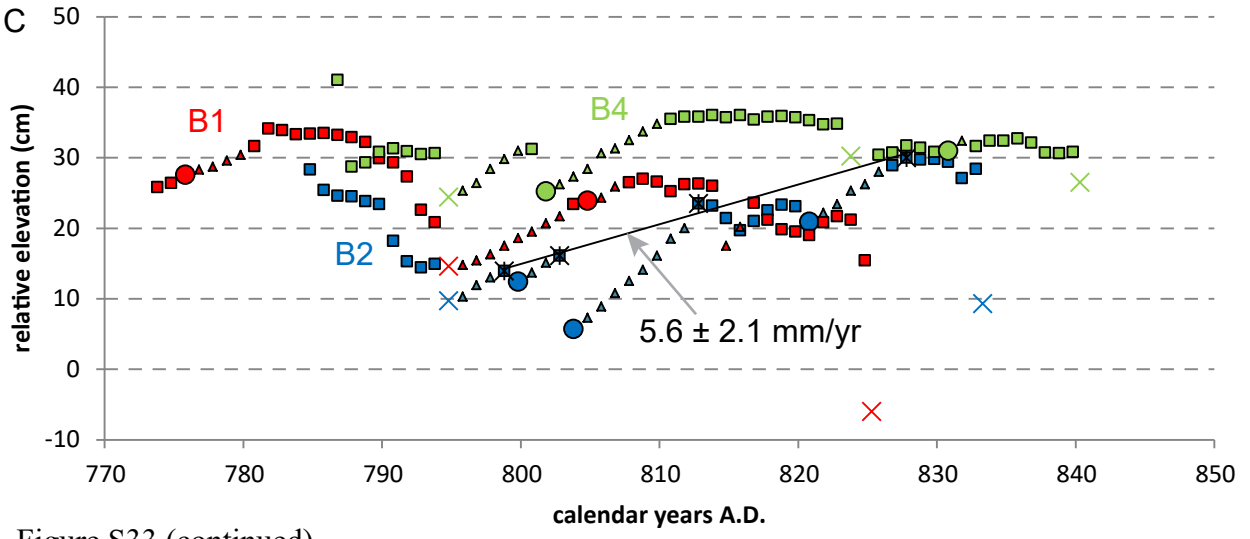

Figure S33 (continued)

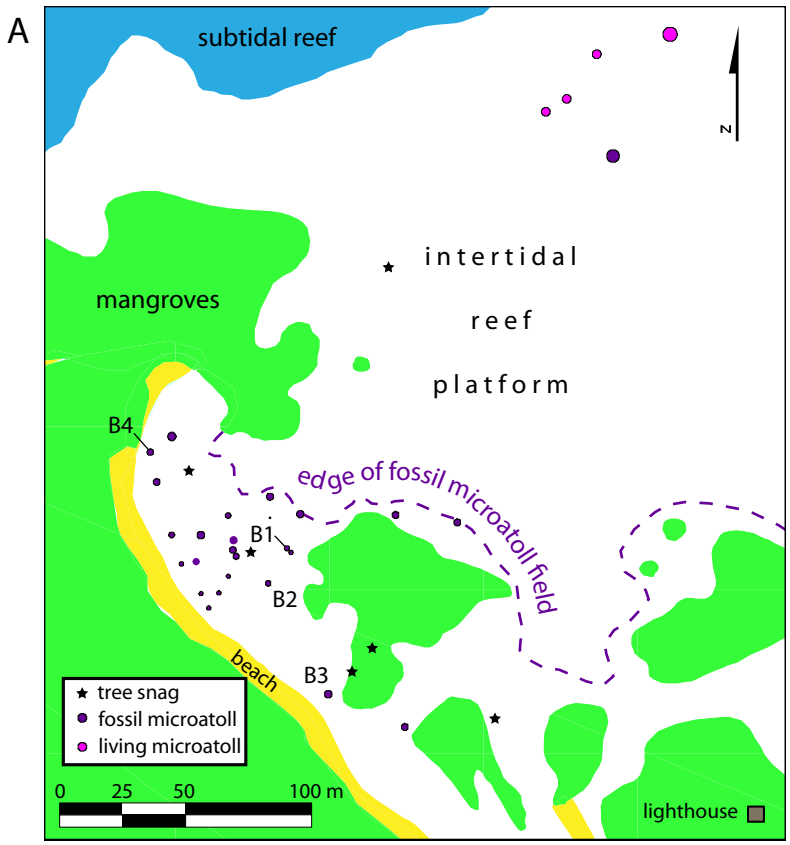

Figure S34. Data from the Sibelua B site. (A) Map of the site on the east coast of South Pagai. A large population of cup-shaped microatolls is clustered near the beach. Slab samples were collected from microatolls B1 and B2 and small chiseled samples (for U-Th dating) were taken from B3 and B4.

(B) Cross sections and (C) growth history plot of B1 and B2 (all symbols as in Fig. S5). The 370 ± 9 and 281 ± 21 ages on B2 are inconsistent with the other four B1/2 ages and probably has underestimated uncertainty. Band years are assigned based on matching together the overall morphology of the two records and considering all of the dates. Both B1 and B2 record 80 years of slow interseismic subsidence before they were killed due to an uplift event in about A.D. 385. The date obtained from B3 suggests a slightly younger age for the uplift event, but uncertainties may well be underestimated for several of these dates. The B4 microatoll was about 20 cm higher than the B1/2/3 population and may represent a different generation. Its age is imprecise, but as one plausible scenario, B4 may have died due to an uplift event in the early 300s, around the time that B1/2 first hit HLS.

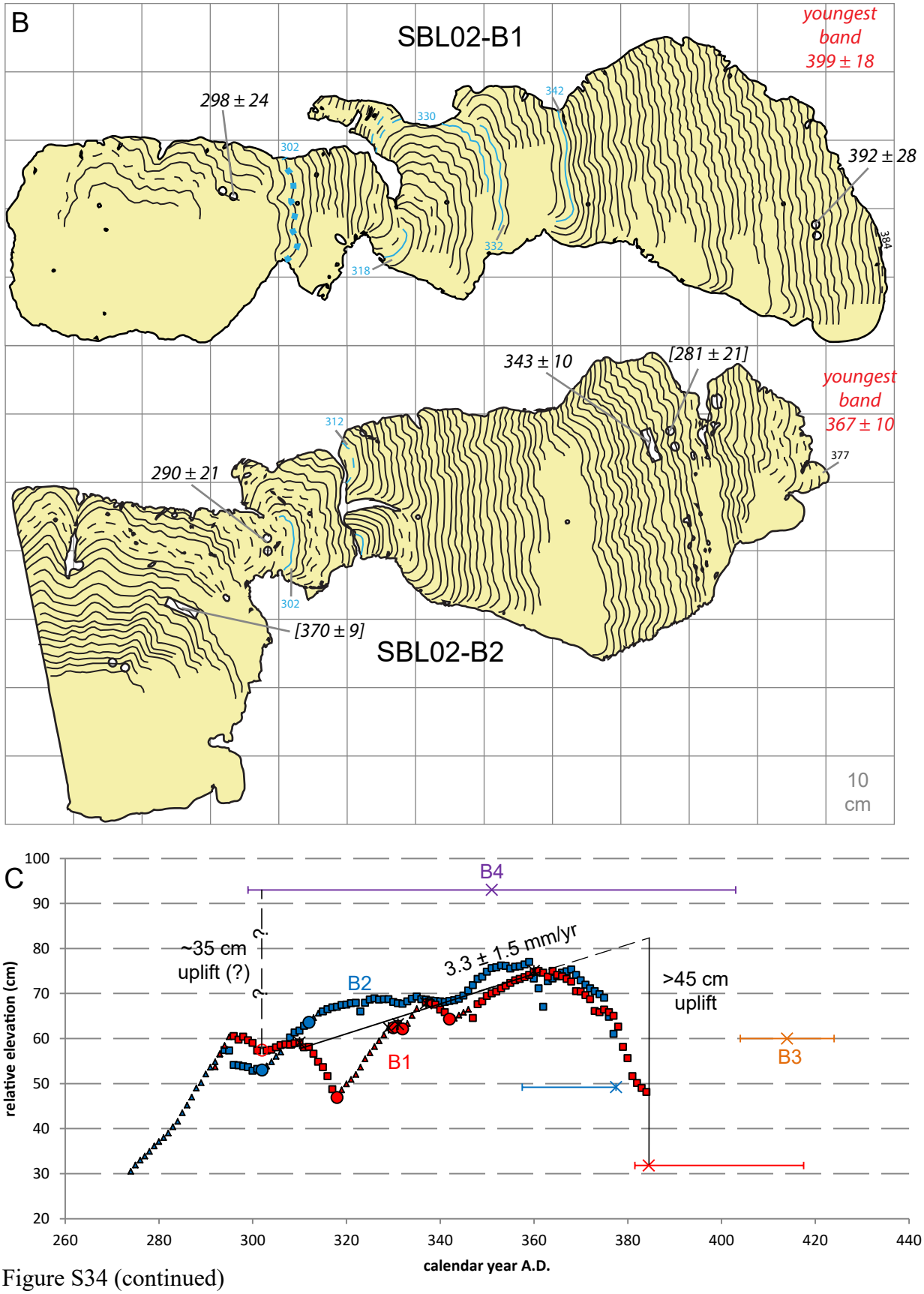

Figure S34 (continued)

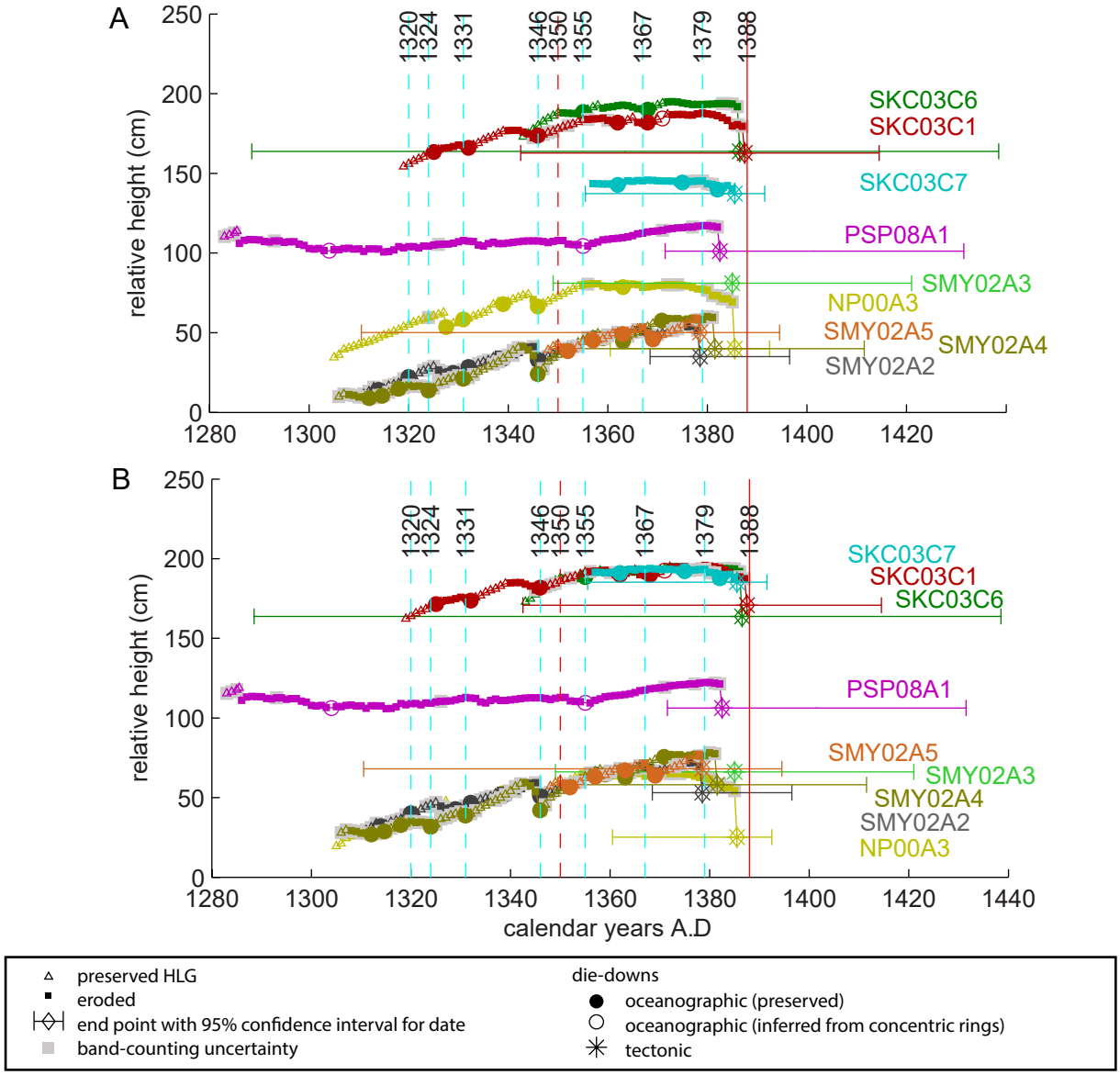

Figure S35. Records of corals that apparently died in a tectonic uplift around 1388, from Sikici (SKC), Pasapuat (PSP), and Simanganya (SMY) sites. Sikici and Simanganya records were originally presented by *Sieh et al.* [2008] and Pasapuat record by *Philibosian et al.* [2012]. Records have been shifted within their age uncertainty based on cross-correlations between sequences of oceanographic die-downs, with the assumption that they all died at the same time but each potentially had a small number of annual bands eroded off the outer perimeter. Vertical dashed blue lines mark dates of strong oceanographic die-downs identified in very precisely dated coral records on Simeulue island (from *Meltzner et al.* [2010, 2012]). Absolute ages of these Mentawai specimens have been assigned by aligning many of their strong die-downs with those recorded in the Simeulue corals, as these were likely basin-wide Indian Ocean Dipole events. (A) Original coral heights; (B) heights shifted upward to correct for presumed settling into the substrate at Sikici and Simanganya. The 1350 event that uplifted corals at several sites farther south is shown for reference with a vertical red dashed line; none of these corals was apparently uplifted at that time.

Table S1. Uranium and thorium isotopic compositions and ^{230}Th ages of coral subsamples by MC-ICPMS with dates A.D.

Subsample	^{238}U ppb	^{232}Th ppt	δ^{234}U measured[a]	[^{230}Th/^{238}U] activity[c]	[^{230}Th/^{232}Th] ppm[d]	Age uncorrected	Age corrected[c,e]	$\delta^{234}U_{initial}$ corrected[b]	$^{230}Th/^{232}Th_{initial}$ ppm[f]	Calendar Year A.D.[h]
SRB10-B3-1	1979.7 ± 3.4	233.1 ± 4.7	144.1 ± 2.5	0.003863 ± 0.000051	542 ± 13	369.3 ± 4.9	364.9 ± 6.6	144.2 ± 2.5		1645.1 ± 6.6
SRB10-B3-2	1929.4 ± 2.4	186.4 ± 8.5	146.2 ± 1.7	0.004303 ± 0.000027	736 ± 34	410.7 ± 2.7	407.1 ± 4.5	146.4 ± 1.7		1605.9 ± 4.5
MSB10-A1-1	2264.2 ± 2.1	26247 ± 98	143.9 ± 1.5	0.00674 ± 0.00020	9.60 ± 0.29	645 ± 19	209 ± 438	144.0 ± 1.6		1801 ± 438
MSB10-A1-2	2397.0 ± 2.3	13353 ± 44	146.7 ± 1.6	0.00548 ± 0.00013	16.25 ± 0.39	523 ± 13	314 ± 210	146.9 ± 1.6		1698 ± 210
MSB10-A1-3	2138.0 ± 2.8	16702 ± 51	148.0 ± 3.7	0.00557 ± 0.00021	11.77 ± 0.45	531 ± 21	238 ± 294	148.1 ± 3.8		1774 ± 294
MSB10-A2-1	2581.3 ± 5.6	527.8 ± 6.4	148.1 ± 2.5	0.004077 ± 0.000055	329.2 ± 6.0	388.4 ± 5.3	380.7 ± 9.3	148.3 ± 2.5		1629.3 ± 9.3
MSB10-A2-2	2785.6 ± 4.9	1275 ± 11	143.8 ± 2.1	0.004128 ± 0.000027	148.9 ± 1.6	394.8 ± 2.7	378 ± 17	144.0 ± 2.1		1635 ± 17
MSB10-A3-1-2	2177.8 ± 4.0	1351.1 ± 7.1	148.0 ± 2.5	0.004002 ± 0.000056	106.5 ± 1.6	381 ± 5.4				
MSB10-A3-1-3	2075.3 ± 3.5	1024.5 ± 6.9	144.8 ± 2.3	0.003950 ± 0.000056	132.1 ± 2.1	377 ± 5.4	375.0 ± 9.0	143.0 ± 5.0	1.8 ± 3.3	1636.0 ± 9.0
MSB10-A3-1-4	2154.8 ± 3.7	524.8 ± 6.8	144.9 ± 2.5	0.003953 ± 0.000054	268.0 ± 5.0	378 ± 5.2				
MSB10-A3-2	2078.3 ± 1.1	438.3 ± 4.7	143.8 ± 1.3	0.004148 ± 0.000019	324.7 ± 3.8	396.7 ± 1.9	388.7 ± 8.2	143.9 ± 1.3		1627.3 ± 8.2
MSB10-A3-3	2191.4 ± 2.6	446 ± 13	145.8 ± 1.6	0.00363 ± 0.00018	294 ± 17	346 ± 17	338 ± 19	146.0 ± 1.6		1675 ± 19
PJG10-A1-1-1	2343.1 ± 7.3	7979 ± 35	145.3 ± 4.1	0.00754 ± 0.00014	36.54 ± 0.69	721 ± 14				
PJG10-A1-1-2	2488.2 ± 2.9	6178 ± 14	146.2 ± 1.8	0.006841 ± 0.000092	45.49 ± 0.62	653.6 ± 8.9	431 ± 23	144.8 ± 4.7	15.3 ± 1.1	1579 ± 23
PJG10-A1-1-3	2401.4 ± 2.7	11732 ± 31	147.6 ± 2.0	0.00908 ± 0.00014	30.69 ± 0.48	867 ± 14				
PJG10-A1-1-4	2391.5 ± 3.0	7999 ± 18	143.3 ± 2.0	0.00768 ± 0.00011	37.89 ± 0.55	735 ± 11				
PJG10-A1-2	2181.3 ± 2.2	867.9 ± 9.6	144.9 ± 1.4	0.005266 ± 0.000031	218.5 ± 2.7	503.4 ± 3.0	488 ± 15	145.1 ± 1.4		1525 ± 15
PJG12-C1-1	1953.8 ± 1.4	2003 ± 16	145.9 ± 1.4	0.004746 ± 0.000052	76.4 ± 1.0	453.2 ± 5.0	415 ± 39	146.0 ± 1.4		1597 ± 39
PJG12-C1-2	2236.5 ± 2.7	3206 ± 18	142.2 ± 1.8	0.005261 ± 0.000069	60.59 ± 0.86	504.1 ± 6.7	450 ± 54	142.4 ± 1.8		1563 ± 54
PJG12-C2-1	1680.8 ± 1.3	200 ± 12	148.0 ± 1.5	0.003729 ± 0.000059	517 ± 32	355.3 ± 5.7	350.8 ± 7.2	148.1 ± 1.5		1661.2 ± 7.2
PJG12-C2-3	2273.9 ± 2.4	534.1 ± 6.4	145.0 ± 1.6	0.004633 ± 0.000020	325.7 ± 4.1	442.7 ± 2.0	433.9 ± 9.0	145.2 ± 1.6		1579.1 ± 9.0
NPK10-A2-1	2165.4 ± 4.3	8936 ± 37	146.7 ± 2.3	0.00521 ± 0.00013	20.84 ± 0.54	497 ± 13	342 ± 155	146.8 ± 2.3		1668 ± 155
NPK10-A2-2-1	2327.5 ± 1.5	8334 ± 22	145.3 ± 1.4	0.00548 ± 0.00009	25.25 ± 0.41	523.4 ± 8.4				
NPK10-A2-2-2	2367.5 ± 1.4	9640 ± 22	145.6 ± 1.3	0.00564 ± 0.00010	22.86 ± 0.41	539 ± 10	430 ± 78	153 ± 12	4.5 ± 3.4	1586 ± 78
NPK10-A2-2-3	2364.4 ± 1.5	9349 ± 22	142.4 ± 1.6	0.00533 ± 0.00010	22.27 ± 0.43	510.9 ± 9.9				
NPK10-A2-2-4	2369.3 ± 1.5	9932 ± 26	143.4 ± 1.4	0.00562 ± 0.00012	22.13 ± 0.49	538 ± 12				
NPK10-A2-3	2044.9 ± 2.2	13274 ± 35	143.7 ± 1.4	0.00694 ± 0.00013	17.64 ± 0.33	664 ± 12	420 ± 245	143.9 ± 1.4		1593 ± 245
NPK10 A2-4	2047.8 ± 1.8	4355 ± 10	147.0 ± 1.5	0.005458 ± 0.000075	42.37 ± 0.59	520.8 ± 7.2	441 ± 80	147.2 ± 1.5		1571 ± 80
NPK10-A2-5	2176.9 ± 2.1	2747 ± 11	145.5 ± 1.4	0.004588 ± 0.000048	60.04 ± 0.68	438.2 ± 4.7	391 ± 48	145.7 ± 1.4		1622 ± 48
SKC08-C2	2449.6 ± 3.0	82.9 ± 3.4	149.4 ± 1.9	0.004422 ± 0.000031	2158 ± 90	420.9 ± 3.1	419.6 ± 3.3	149.6 ± 1.9		1588.4 ± 3.3
SKC08-C5	2381.8 ± 2.9	141.1 ± 3.9	144.7 ± 2.1	0.004508 ± 0.000038	1256 ± 37	430.8 ± 3.7	428.6 ± 4.3	144.9 ± 2.1		1579.4 ± 4.3
PSP08-B1-1	2280.2 ± 1.8	1142.9 ± 6.4	143.9 ± 1.4	0.003882 ± 0.000053	127.9 ± 1.9	371.2 ± 5.1	352 ± 20	144.1 ± 1.4		1656 ± 20
PSP08-B1-2	2338.1 ± 1.5	702.1 ± 6.6	145.6 ± 1.3	0.003859 ± 0.000049	212.2 ± 3.4	368.5 ± 4.7	357 ± 12	145.8 ± 1.3		1651 ± 12
PSP08-B1-3	2372.2 ± 3.6	862.9 ± 7.5	144.5 ± 2.1	0.003990 ± 0.000063	181.1 ± 3.2	381.3 ± 6.0	368 ± 15	144.6 ± 2.1		1641 ± 15
PSP08-B2-1	2332.2 ± 1.6	1820.9 ± 7.0	147.3 ± 1.4	0.004492 ± 0.000062	95.0 ± 1.4	428.3 ± 5.9	399 ± 30	147.5 ± 1.4		1609 ± 30
PSP08-B2-2	2718.3 ± 1.3	2433 ± 11	148.1 ± 1.4	0.004685 ± 0.000038	86.44 ± 0.80	446.5 ± 3.7	413 ± 34	148.2 ± 1.4		1603 ± 34
PSP08-B2-3	2804.4 ± 2.9	8539 ± 24	145.3 ± 1.5	0.006398 ± 0.000086	34.69 ± 0.47	611.7 ± 8.3	497 ± 115	145.5 ± 1.5		1516 ± 115
PSP08-B3-1-1	2426.4 ± 1.5	5722 ± 11	146.7 ± 1.3	0.005255 ± 0.000086	36.79 ± 0.61	501.5 ± 8.3				
PSP08-B3-1-2	2449.5 ± 2.8	6369 ± 16	145.6 ± 1.8	0.005410 ± 0.000076	34.35 ± 0.49	516.8 ± 7.3	368 ± 31	148.0 ± 6.7	9.99 ± 2.00	1640 ± 31
PSP08-B3-1-3	2429.8 ± 2.6	5865 ± 13	147.5 ± 1.7	0.005371 ± 0.000074	36.73 ± 0.51	512.2 ± 7.2				
PSP08-B3-1-4	2497.1 ± 2.8	8079 ± 18	146.4 ± 1.8	0.005827 ± 0.000087	29.74 ± 0.45	556.4 ± 8.3				
PSP08-B3-2	1530.9 ± 1.6	3829.1 ± 9.7	146.1 ± 1.6	0.006269 ± 0.000073	41.38 ± 0.49	598.8 ± 7.0	505 ± 94	146.3 ± 1.6		1508 ± 94
PSP08-B3-3	2269.2 ± 2.4	9301 ± 27	143.0 ± 1.5	0.00731 ± 0.00012	29.44 ± 0.50	700 ± 12	546 ± 155	143.2 ± 1.6		1467 ± 155
PSP08-B4-2	2107.9 ± 1.9	29.2 ± 5.7	146.0 ± 1.5	0.003998 ± 0.000053	4765 ± 936	381.6 ± 5.1	381.1 ± 5.1	146.2 ± 1.5		1627.9 ± 5.1

Subsample	^{238}U ppb	^{232}Th ppt	$\delta^{234}U$ measured[a]	$[^{230}Th/^{238}U]$ activity[c]	$[^{230}Th/^{232}Th]$ ppm[d]	Age uncorrected	Age corrected [c,e]	$\delta^{234}U_{initial}$ corrected[b]	$^{230}Th/^{232}Th_{initial}$ ppm[f]	Calendar Year A.D.[h]
CMP08-A1-1-1	2302.3 ± 2.4	3848 ± 14	142.9 ± 1.6	0.004491 ± 0.000077	44.36 ± 0.78	429.9 ± 7.4				
CMP08-A1-1-2	2393.0 ± 2.3	3220 ± 11	145.2 ± 1.8	0.004441 ± 0.000071	54.50 ± 0.89	424.3 ± 6.8	400 ± 28	145.0 ± 7.8	2.70 ± 10.26	1608 ± 28
CMP08-A1-1-3	2444.0 ± 2.0	4621 ± 11	145.2 ± 1.6	0.004528 ± 0.000065	39.54 ± 0.58	432.5 ± 6.3				
CMP08-A1-3	2443.2 ± 2.5	4419 ± 14	144.9 ± 1.5	0.004708 ± 0.000068	42.98 ± 0.64	449.9 ± 6.6	382 ± 68	145.1 ± 1.5		1631 ± 68
CMP08-A2-2-1	2706.2 ± 3.8	48721 ± 310	145.8 ± 2.2	0.00515 ± 0.00027	4.72 ± 0.25	492 ± 26				
CMP08-A2-2-2	2827.1 ± 3.0	33997 ± 167	144.3 ± 1.7	0.00446 ± 0.00022	6.13 ± 0.30	427 ± 21	294 ± 77	149.2 ± 8.1	1.8 ± 2.0[g]	1718 ± 129[g]
CMP08-A2-2-3	2656.1 ± 1.9	23073 ± 89	146.3 ± 1.5	0.00391 ± 0.00018	7.44 ± 0.34	373 ± 17				
CMP08-A2-2-4	2745.6 ± 2.2	25967 ± 115	146.1 ± 1.7	0.00435 ± 0.00015	7.59 ± 0.27	415 ± 14				
CMP08-A2-3	2348.2 ± 4.5	4951 ± 12	148.6 ± 2.2	0.003754 ± 0.000095	29.40 ± 0.75	357.5 ± 9.1	279 ± 79	148.7 ± 2.2		1730 ± 79
CMP08-A2-4	2462.2 ± 6.7	4005 ± 22	140.9 ± 3.6	0.003877 ± 0.000085	39.35 ± 0.88	371.7 ± 8.2	310 ± 62	141.1 ± 3.6		1702 ± 62
CMP08-A3-1-1	2529.3 ± 2.1	5651 ± 13	146.9 ± 1.5	0.004468 ± 0.000083	33.02 ± 0.62	426.2 ± 8.0				
CMP08-A3-1-3	2632.0 ± 2.7	8203 ± 17	147.3 ± 1.8	0.004647 ± 0.000075	24.62 ± 0.40	443.2 ± 7.2	390 ± 23	148.9 ± 4.7	2.86 ± 1.19	1618 ± 23
CMP08-A3-1-4	2558.5 ± 2.6	9812 ± 22	145.6 ± 1.8	0.004743 ± 0.000080	20.42 ± 0.35	453.0 ± 7.7				
CMP08-A3-2	2593.7 ± 2.7	15051 ± 46	147.2 ± 1.5	0.00559 ± 0.00011	15.92 ± 0.31	534 ± 10	316 ± 218	147.3 ± 1.5		1697 ± 218
CMP08-B1-1	2382.3 ± 2.6	1239.0 ± 4.4	145.0 ± 1.8	0.003844 ± 0.000039	122.0 ± 1.3	367.2 ± 3.8	348 ± 20	145.1 ± 1.8		1660 ± 20
CMP08-B1-2	2680.7 ± 3.2	699 ± 10	145.5 ± 1.7	0.004922 ± 0.000025	311.7 ± 4.8	470.1 ± 2.5	460 ± 10	145.7 ± 1.7		1553 ± 10
CMP08-B2-1-1	2113.4 ± 1.7	2554.7 ± 8.6	144.8 ± 1.5	0.004533 ± 0.000065	61.92 ± 0.91	433.2 ± 6.3				
CMP08-B2-1-2	2361.1 ± 2.2	1986.0 ± 7.6	145.2 ± 1.7	0.004461 ± 0.000054	87.6 ± 1.1	426.1 ± 5.2	408 ± 21	146.0 ± 6.5	3.46 ± 3.67	1600 ± 21
CMP08-B2-1-3	2359.2 ± 2.5	2239.9 ± 7.9	145.0 ± 1.8	0.004453 ± 0.000058	77.4 ± 1.0	425.5 ± 5.6				
CMP08-B2-2	2328.0 ± 2.9	5564 ± 16	147.8 ± 1.9	0.004793 ± 0.000074	33.11 ± 0.52	456.9 ± 7.1	367 ± 90	148.0 ± 1.9		1646 ± 90
CMP08-B3-1	2385.4 ± 2.2	6835 ± 23	146.7 ± 1.6	0.00514 ± 0.00011	29.63 ± 0.65	491 ± 11	383 ± 108	146.9 ± 1.6		1625 ± 108
CMP08-B3-2	2382.2 ± 3.0	4522 ± 13	147.6 ± 1.9	0.005135 ± 0.000072	44.66 ± 0.64	489.6 ± 7.0	419 ± 71	147.8 ± 1.9		1594 ± 71
CMP08-B4-1-1	2394.7 ± 1.6	8544 ± 32	144.2 ± 1.2	0.00475 ± 0.00011	21.96 ± 0.53	454 ± 11				
CMP08-B4-1-2	2436.5 ± 2.6	5030 ± 13	144.3 ± 1.8	0.004790 ± 0.000066	38.31 ± 0.54	458 ± 6.4	451 ± 12	148.0 ± 3.2	0.16 ± 2.22	1557 ± 12
CMP08-B4-1-3	2501.7 ± 3.0	4663 ± 12	147.2 ± 2.0	0.004792 ± 0.000068	42.45 ± 0.61	457 ± 6.5				
CMP08-B4-1-4	2362.6 ± 2.7	3969.6 ± 8.8	146.5 ± 1.9	0.004715 ± 0.000055	46.33 ± 0.55	450 ± 5.3				
CMP08-B4-2	2348.4 ± 2.9	1387.5 ± 9.9	144.8 ± 1.9	0.004783 ± 0.000032	133.7 ± 1.3	457.1 ± 3.2	435 ± 22	145.0 ± 1.9		1578 ± 22
CMP08-B4-3-1	2185.2 ± 1.2	2941 ± 10	146.9 ± 1.6	0.004621 ± 0.000052	56.69 ± 0.67	440.8 ± 5.1				
CMP08-B4-3-2	2432.6 ± 1.5	6771 ± 14	149.2 ± 1.2	0.004678 ± 0.000077	27.75 ± 0.46	445.4 ± 7.4	434 ± 10	142.8 ± 2.6	0.81 ± 0.97	1582 ± 10
CMP08-B4-3-3	2454.2 ± 7.7	3600 ± 10	140.4 ± 5.2	0.004607 ± 0.000058	51.86 ± 0.65	442.0 ± 5.9				
CMP08-B4-3-4	2369.4 ± 1.5	3687 ± 11	145.5 ± 1.7	0.004590 ± 0.000058	48.71 ± 0.63	438.4 ± 5.6				
CMP08-B5	2295.2 ± 2.0	155.2 ± 3.3	144.4 ± 1.7	0.004240 ± 0.000032	1035 ± 23	405.3 ± 3.1	402.8 ± 4.0	144.6 ± 1.7		1605.2 ± 4.0
CMP08-C1-1-1	2386.2 ± 2.3	9541 ± 34	145.3 ± 1.7	0.00469 ± 0.00011	19.37 ± 0.48	448 ± 11				
CMP08-C1-1-2	2511.2 ± 2.5	20951 ± 60	147.1 ± 1.9	0.00502 ± 0.00011	9.94 ± 0.22	479 ± 10	423 ± 14	143.8 ± 3.5	1.18 ± 0.45	1585 ± 14
CMP08-C1-1-4	2551.2 ± 2.7	9453 ± 23	145.1 ± 1.8	0.004699 ± 0.000078	20.94 ± 0.35	449.0 ± 7.5				
CMP08-C1-2	2411.0 ± 2.7	1824.4 ± 9.7	148.0 ± 1.6	0.004809 ± 0.000038	104.9 ± 1.0	458.4 ± 3.7	430 ± 29	148.1 ± 1.7		1583 ± 29
CMP08-C2-1	2242.4 ± 2.0	1597.0 ± 5.7	145.1 ± 1.5	0.004461 ± 0.000053	103.4 ± 1.3	426 ± 5.1	399 ± 27	145.3 ± 1.5		1609 ± 27
CMP08-C2-2	2272.3 ± 2.4	1474 ± 11	147.1 ± 1.4	0.005263 ± 0.000039	134.0 ± 1.4	502.1 ± 3.8	478 ± 25	147.3 ± 1.4		1535 ± 25
PCB08-B1-1	2161.8 ± 2.9	432.3 ± 6.3	148.7 ± 1.9	0.003492 ± 0.000061	288.4 ± 6.5	332.5 ± 5.8	325.0 ± 9.5	148.8 ± 2.0		1684.0 ± 9.5
PCB08-B1-4	2274.7 ± 2.6	493.8 ± 9.9	147.2 ± 1.8	0.004627 ± 0.000026	351.9 ± 7.3	441.3 ± 2.6	433.1 ± 8.5	147.3 ± 1.8		1579.9 ± 8.5
PCB08-B1-5	2295.0 ± 3.2	2589.9 ± 9.9	145.5 ± 2.1	0.005338 ± 0.000072	78.1 ± 1.1	510.0 ± 6.9	468 ± 43	145.7 ± 2.1		1543 ± 43
KBG08-A1	2048.3 ± 2.3	185.8 ± 7.3	147.4 ± 1.7	0.001993 ± 0.000061	363 ± 18	189.9 ± 5.8	186.5 ± 6.8	147.5 ± 1.7		1822.5 ± 6.8
KBG10-B1-1	2434.9 ± 3.9	547.7 ± 7.2	146.6 ± 2.1	0.003466 ± 0.000052	254.4 ± 5.1	330.6 ± 5.0	322 ± 10	146.7 ± 2.1		1688 ± 10
KBG10-B1-2	2533.0 ± 3.4	901 ± 10	144.5 ± 1.9	0.003918 ± 0.000024	181.9 ± 2.4	374.4 ± 2.4	361 ± 14	144.7 ± 1.9		1652 ± 14
KBG10-B2-1-1	2481.0 ± 5.1	6893 ± 33	146.9 ± 2.5	0.00471 ± 0.00010	28.00 ± 0.62	449.5 ± 9.8				
KBG10-B2-1-2	2428.0 ± 1.9	7042 ± 16	150.3 ± 1.6	0.004712 ± 0.000090	26.82 ± 0.52	448.2 ± 8.6	316 ± 61	148 ± 11	7.9 ± 5.8[g]	1695 ± 104[g]
KBG10-B2-1-3	2399.9 ± 1.9	10107 ± 25	148.1 ± 1.6	0.00533 ± 0.00011	20.89 ± 0.44	508 ± 11				
KBG10-B2-1-4	2408.6 ± 1.7	6401 ± 15	147.3 ± 1.6	0.004536 ± 0.000098	28.18 ± 0.61	432.5 ± 9.4				
SGK10-A3-1	2585.9 ± 5.4	112.0 ± 6.2	145.8 ± 2.4	0.003491 ± 0.000053	1331 ± 76	333.2 ± 5.1	331.5 ± 5.4	145.9 ± 2.4		1678.5 ± 5.4
SDG10-A1-1	2345.7 ± 5.5	91.2 ± 6.0	147.5 ± 2.9	0.003488 ± 0.000054	1480 ± 100	332.4 ± 5.2	330.9 ± 5.4	147.7 ± 2.9		1679.1 ± 5.4
SDG10-A1-3	2493.2 ± 3.5	124.3 ± 6.7	147.2 ± 2.0	0.004279 ± 0.000019	1417 ± 76	408.0 ± 2.0	406.1 ± 2.7	147.4 ± 2.0		1607 ± 2.7
SDG10-A2-1	2769.7 ± 9.4	227.8 ± 5.7	147.9 ± 3.9	0.004040 ± 0.000050	811 ± 22	385.0 ± 4.9	381.9 ± 5.8	148.1 ± 4.0		1628.1 ± 5.8
SDG10-A2-2	2411.8 ± 3.2	98 ± 14	148.6 ± 2.1	0.004492 ± 0.000036	1834 ± 265	427.8 ± 3.6	426.3 ± 3.9	148.8 ± 2.1		1586.7 ± 3.9

Subsample	^{238}U ppb	^{232}Th ppt	$\delta^{234}U$ measured[a]	$[^{230}Th/^{238}U]$ activity[c]	$[^{230}Th/^{232}Th]$ ppm[d]	Age uncorrected	Age corrected [c,e]	$\delta^{234}U_{initial}$ corrected[b]	$^{230}Th/^{232}Th_{initial}$ ppm[f]	Calendar Year A.D.[h]
SLG10-B1-1	2847.8 ± 1.9	7540 ± 16	147.5 ± 1.2	0.01559 ± 0.00014	97.19 ± 0.91	1493 ± 14	1394 ± 100	148.1 ± 1.2		617 ± 100
SLG10-B1-2	2941.6 ± 4.3	4272 ± 14	146.8 ± 2.1	0.01441 ± 0.00011	163.8 ± 1.4	1380 ± 11	1326 ± 56	147.4 ± 2.1		687 ± 56
SLG10-B2-1	2352.0 ± 2.8	55.6 ± 6.4	144.0 ± 1.9	0.013929 ± 0.000063	9723 ± 1120	1337.3 ± 6.5	1336.5 ± 6.6	144.6 ± 1.9		673.5 ± 6.6
TLU10-A1-1-1	2439.5 ± 6.5	16582 ± 91	146.6 ± 3.5	0.01683 ± 0.00029	40.88 ± 0.74	1614 ± 29				
TLU10-A1-1-2	2359.0 ± 3.3	25845 ± 87	148.5 ± 2.2	0.01785 ± 0.00031	26.91 ± 0.47	1710 ± 30	1430 ± 74	145.0 ± 7.3	4.3 ± 2.8	581 ± 74
TLU10-A1-1-3	2410.8 ± 3.5	24323 ± 81	145.3 ± 2.2	0.01740 ± 0.00030	28.47 ± 0.50	1671 ± 29				
TLU10-A1-1-4	2394.9 ± 3.7	17952 ± 59	146.6 ± 2.3	0.01665 ± 0.00028	36.67 ± 0.62	1597 ± 27				
TLU10-A1-2	2258.2 ± 3.4	58713 ± 288	144.5 ± 2.0	0.02062 ± 0.00047	13.09 ± 0.31	1984 ± 46	1004 ± 986	144.9 ± 2.0		1009 ± 986
SSB10-A1-1	2730.7 ± 4.8	698.9 ± 7.2	146.4 ± 2.0	0.01556 ± 0.00011	1004 ± 12	1492 ± 11	1482 ± 15	147.0 ± 2.0		528 ± 15
SSB10-A1-2	2391.5 ± 3.8	339.7 ± 8.1	145.7 ± 2.1	0.015217 ± 0.000049	1769 ± 42	1460 ± 5.4	1454 ± 7.6	146.3 ± 2.1		558.7 ± 7.6
SSB10-A1-4	2234.3 ± 1.2	301.0 ± 3.7	144.9 ± 1.2	0.015281 ± 0.000030	1873 ± 23	1467 ± 3.3	1462 ± 6.0	145.5 ± 1.2		554.1 ± 6.0
SSB10-A2-1	2791.7 ± 6.3	1685 ± 45	147.8 ± 2.6	0.01569 ± 0.00010	429 ± 12	1503 ± 10	1480 ± 25	148.4 ± 2.6		530 ± 25
SSB10-A2-3	2891.1 ± 4.1	1621 ± 15	145.0 ± 1.9	0.015663 ± 0.000077	461.1 ± 4.9	1503.7 ± 7.9	1483 ± 22	145.6 ± 1.9		530 ± 22
SSB10-A2-4	2364.1 ± 1.8	1887 ± 9.8	143.3 ± 1.6	0.01540 ± 0.00007	319 ± 2.3	1481 ± 7.5	1451 ± 31	143.8 ± 1.6		565 ± 31
BSA03-B1-1a	2380.0 ± 4.0	43170 ± 170	144.8 ± 1.9	0.017560 ± 0.000330	16.0 ± 0.3	1687.0 ± 32	1000 ± 690	145.3 ± 2.0		1004 ± 690
BSA03-B1-new1	2567.7 ± 1.8	14168 ± 284	145.8 ± 1.3	0.014327 ± 0.000064	42.9 ± 0.9	1373.7 ± 6.3	1164 ± 230	146.3 ± 1.3		852 ± 230
BSA03-B1-new2A	2335.8 ± 2.0	4022 ± 81	146.1 ± 1.3	0.013857 ± 0.000054	132.9 ± 2.7	1328.1 ± 5.4				
BSA03-B1-new2B	2420.4 ± 2.0	6128 ± 123	145.0 ± 1.3	0.014248 ± 0.000061	92.9 ± 1.9	1366.9 ± 6.1				
BSA03-B1-new2C	2478.7 ± 2.1	17519 ± 351	146.7 ± 1.4	0.015180 ± 0.000060	35.5 ± 0.7	1454.9 ± 6.0	1294 ± 27	145.0 ± 21.0	4.0 ± 0.4	722 ± 27
BSA03-B1-new2D	2559.3 ± 2.3	31136 ± 623	145.6 ± 1.3	0.016438 ± 0.000069	22.3 ± 0.5	1577.7 ± 6.9				
BSA03-B1-new2	2295.4 ± 1.9	4346 ± 87	147.1 ± 1.3	0.013872 ± 0.000067	121.0 ± 2.5	1328.4 ± 6.7				
BSA03-B2a-2a	2275.0 ± 4.0	24420 ± 80	150.0 ± 1.8	0.01461 ± 0.00021	22.50 ± 0.30	1396 ± 21	1000 ± 400	150.5 ± 1.8		1004 ± 400
BSA03-B2b-1a	2389.0 ± 3.0	13447 ± 30	147.8 ± 1.7	0.01325 ± 0.00012	38.90 ± 0.40	1268 ± 12	1060 ± 210	148.2 ± 1.7		944 ± 210
BSA03-B3-2a	2223.0 ± 3.0	10835 ± 30	151.5 ± 1.7	0.016570 ± 0.00015	56.10 ± 0.50	1582 ± 15	1400 ± 180	152.1 ± 1.7		604 ± 180
BSA03-B4-1b	2269.0 ± 4.0	88600 ± 370	146.9 ± 1.7	0.020630 ± 0.00049	8.70 ± 0.20	1980 ± 50	510 ± 1490	147.1 ± 1.8		1494 ± 1490
BSA03-B4-new1A	2462.4 ± 2.1	18790 ± 376	147.1 ± 1.4	0.014043 ± 0.00005	30.39 ± 0.62	1345 ± 5.5				
BSA03-B4-new1B	2608.1 ± 2.3	39419 ± 789	147.6 ± 1.4	0.015655 ± 0.00005	17.10 ± 0.35	1499 ± 5.5				
BSA03-B4-new1C	2480.3 ± 2.0	43437 ± 870	145.3 ± 1.3	0.016074 ± 0.00005	15.15 ± 0.31	1543 ± 4.9	1228 ± 35	145.0 ± 26.0	3.1 ± 0.3	788 ± 35
BSA03-B4-new1D	2545.7 ± 2.4	110141 ± 2205	146.8 ± 1.3	0.020752 ± 0.00006	7.92 ± 0.16	1993 ± 6.3				
BSA03-B4-new1	2640.3 ± 2.1	18209 ± 365	145.3 ± 1.4	0.014139 ± 0.00007	33.85 ± 0.70	1356 ± 6.8				
BSA03-B4-new1R	2387.3 ± 1.7	23787 ± 476	145.8 ± 1.3	0.014887 ± 0.00007	24.67 ± 0.51	1428 ± 7.2				
BSA03-B4-new2	2505.2 ± 1.8	21255 ± 425	148.0 ± 1.2	0.014105 ± 0.00009	27.45 ± 0.58	1350 ± 9.0	1032 ± 450	148.47 ± 1.3		984 ± 450
BSA03-B4-new3	2432.7 ± 2.2	20705 ± 415	148.5 ± 1.3	0.013849 ± 0.00007	26.87 ± 0.55	1326 ± 7.0	1110 ± 153	148.936 ± 1.3		906 ± 153
SBL02-B1-1a	2070.4 ± 1.7	1459.5 ± 2.8	146.1 ± 1.2	0.017060 ± 0.000085	399.6 ± 2.1	1637.2 ± 8.4	1611 ± 28	146.7 ± 1.2		392 ± 28
SBL02-B1-2b	2123.7 ± 2.8	1235.4 ± 2.4	144.3 ± 1.7	0.017957 ± 0.000087	509.7 ± 2.6	1726.7 ± 8.8	1705 ± 24	145.0 ± 1.7		298 ± 24
SBL02-B2-1a	2381.4 ± 2.0	1239.1 ± 2.7	145.5 ± 1.2	0.018128 ± 0.000088	575.3 ± 3.0	1741.3 ± 8.7	1722 ± 21	146.2 ± 1.2		281 ± 21
SBL02-B2-2a	2470.5 ± 3.4	1285.7 ± 2.7	144.9 ± 1.5	0.018032 ± 0.000076	572.1 ± 2.6	1733.0 ± 7.7	1713 ± 21	145.6 ± 1.5		290 ± 21
SBL02-B2-new1	2777.7 ± 2.2	372.1 ± 7.7	144.5 ± 1.4	0.017175 ± 0.000051	2116.6 ± 44	1650.6 ± 5.3	1646 ± 9	145.2 ± 1.4		370 ± 9
SBL02-B2-new2	2419.9 ± 2.2	278.4 ± 6.4	143.7 ± 1.5	0.017439 ± 0.000078	2502.9 ± 59	1677.3 ± 7.9	1673 ± 10	144.4 ± 1.6		343 ± 10
SBL02-B3-1a	2454.6 ± 2.1	374.9 ± 1.9	144.9 ± 1.3	0.016602 ± 0.000080	1794 ± 12	1594.5 ± 7.9	1589 ± 10	145.6 ± 1.3		414 ± 10
SBL02-B4-1b	2402.5 ± 1.9	3286.4 ± 4.4	146.0 ± 1.0	0.017837 ± 0.000074	215.29 ± 0.93	1712.4 ± 7.4	1661 ± 52	146.7 ± 1.1		342 ± 52

Subsample	^{238}U ppb	^{232}Th ppt	$\delta^{234}U$ measured[a]	$[^{230}Th/^{238}U]$ activity[c]	$[^{230}Th/^{232}Th]$ ppm[d]	Age uncorrected	Age corrected [c,e]	$\delta^{234}U_{initial}$ corrected[b]	$^{230}Th/^{232}Th_{initial}$ ppm[f]	Calendar Year A.D.[h]

Analytical errors are 2σ of the mean. Alternating gray and white shading groups analyses of single annual band samples. Samples highlighted in yellow were eliminated based on inconsistencies with other dates.

[a] $\delta^{234}U = ([^{234}U/^{238}U]_{activity} - 1) \times 1000$.

[b] $\delta^{234}U_{initial}$ corrected was calculated based on ^{230}Th age (T), i.e., $\delta^{234}U_{initial} = \delta^{234}U_{measured} X\ e^{\lambda 234 * T}$, and T is corrected age.

[c] $[^{230}Th/^{238}U]_{activity} = 1 - e^{-\lambda_{230} T} + (\delta^{234}U_{measured}/1000)[\lambda_{230}/(\lambda_{230} - \lambda_{234})](1 - e^{-(\lambda_{230} - \lambda_{234}) T})$, where T is the age.
Decay constants are 9.1577×10^{-6} yr^{-1} for ^{230}Th, 2.8263×10^{-6} yr^{-1} for ^{234}U [*Cheng et al.*, 2000], and 1.55125×10^{-10} yr^{-1} for ^{238}U [*Jaffey et al.*, 1971].

[d] The degree of detrital ^{230}Th contamination is indicated by the $[^{230}Th/^{232}Th]$ atomic ratio instead of the activity ratio.

[e] Age corrections were calculated using an estimated atomic $^{230}Th/^{232}Th$ ratio of 6.5 ± 6.5 ppm [*Zachariasen et al.*, 1999].

[f] For certain samples, more precise ages, $\delta^{234}U_{initial}$, and $^{230}Th/^{232}Th_{initial}$ values were derived from isochron techniques using an Excel macro, *Isoplot* 3.00 [*Ludwig and Titterington*, 1994; *Ludwig*, 2003].

[g] For isochron regressions with a p-value < 0.05, we increase the uncertainty of both the $^{230}Th/^{232}Th_{initial}$ and the age by a factor of the square root of the mean square of weighted deviates (MSWD), as suggested by *Ludwig* [2003].

[h] Calculated by subtracting the corrected sample age from the year of chemical analysis.

References

Cheng, H., R. L. Edwards, J. Hoff, C. D. Gallup, D. A. Richards, and Y. Asmerom (2000), The half-lives of uranium-234 and thorium-230, *Chemical Geology*, *169*, 17-33.

Jaffey, A. H., K. F. Flynn, L. E. Glendenin, W. C. Bentley, and A. M. Essling (1971), Precision measurements of half-lives and specific activities of ^{235}U and ^{238}U, *Physical Review C*, *4*, 1889-1906.

Ludwig, K. R. (2003), Mathematical–statistical treatment of data and errors for $^{230}Th/U$ geochronology, *Reviews in Mineralogy and Geochemistry*, *52* (1), 631-656.

Ludwig, K. R., and D. M. Titterington (1994), Calculation of $^{230}Th/U$ isochrons, ages, and errors, *Geochim. Cosmochim. Acta, 58* (22), 5031-5042.

Zachariasen, J., K. Sieh, F. W. Taylor, R. L. Edwards, and W. S. Hantoro (1999), Submergence and uplift associated with the giant 1833 Sumatran subduction earthquake: Evidence from coral microatolls, *J. Geophys. Res.*, *104* (B1), 895-919.

Table S2. Reduced Chi-Squared, Moment, and Moment Magnitude for Coseismic Models

	pinned below trench			free below trench		
Model	χ^2_r	M_0 (N m)	M_w	χ^2_r	M_0 (N m)	M_w
1597	0.02	3.7×10^{21}	8.31	0.02	4.2×10^{21}	8.35
1613	0.36	3.3×10^{21}	8.28	0.36	4.7×10^{21}	8.38
1631	0.09	2.3×10^{21}	8.17	0.08	3.5×10^{21}	8.29
1658	0.08	4.1×10^{21}	8.34	0.08	4.8×10^{21}	8.39
1703	0.89	8.2×10^{21}	8.54	0.93	9.4×10^{21}	8.58

Table S3. Reduced Chi-Squared and Moment Deficit Rate for Interseismic Models

Model	χ^2_r	M_0/yr
1520–1580	0.15	3.6×10^{19}
1580–1650	0.53	6.9×10^{19}
1650–1702	0.16	6.2×10^{19}

Movie S1. Continuous animation of interseismic and coseismic megathrust slip from 1520–1703. In the upper image, red and blue areas represent slip deficit and excess, respectively, relative to the assumed plate rate of 4.5 cm/yr of slip starting in 1520. Coseismic slip contours at 50 cm intervals appear for a brief period after each inferred earthquake. The lower graph shows a plot of the relative slip deficit over time with the sweeping vertical line tracking the time of the upper image.